galaxies

MDPI

Review

A Review of Recent Observations of Galactic Winds Driven by Star Formation

David S. N. Rupke

Department of Physics, Rhodes College, Memphis, TN 38112, USA; drupke@gmail.com

Received: 14 September 2018; Accepted: 5 December 2018; Published: 9 December 2018



Abstract: Galaxy-scale outflows of gas, or galactic winds (GWs), driven by energy from star formation are a pivotal mechanism for regulation of star formation in the current model of galaxy evolution. Observations of this phenomenon have proliferated through the wide application of old techniques on large samples of galaxies, the development of new methods, and advances in telescopes and instrumentation. I review the diverse portfolio of direct observations of stellar GWs since 2010. Maturing measurements of the ionized and neutral gas properties of nearby winds have been joined by exciting new probes of molecular gas and dust. Low-z techniques have been newly applied in large numbers at high z. The explosion of optical and near-infrared 3D imaging spectroscopy has revealed the complex, multiphase structure of nearby GWs. These observations point to stellar GWs being a common feature of rapidly star-forming galaxies throughout at least the second half of cosmic history, and suggest that scaling relationships between outflow and galaxy properties persist over this period. The simple model of a modest-velocity, biconical flow of multiphase gas and dust perpendicular to galaxy disks continues to be a robust descriptor of these flows.

Keywords: galactic winds; feedback; outflows; star formation

arXiv:1812.05184v1 [astro-ph.GA] 12 Dec 2018

1. Introduction

Significant amounts of gas in galaxies move in outward radial trajectories due to energy imparted by star formation. This energy originates from a combination of phenomena rooted in stellar processes: radiation, winds, explosive events, and cosmic rays. These gas outflows powered by star formation, or stellar galactic winds (GWs), continue to be a dynamic topic of observational research in the era of large galaxy surveys and multi-messenger astronomy. Outflows are challenging to characterize largely because of two factors: the large contrast between the outflow and an underlying galaxy disk; and the complex, multiphase structure of outflows. High quality data in many gas tracers are essential to adequately quantify the mass, momentum, and energy budget of the wind.

Advances in observations of GWs driven by stellar processes in this decade have come from the use of new observational techniques and the application of old techniques to much larger samples. Both have been aided by new-and-improved telescopes or instrumentation. In the first category fall molecular gas transitions newly applied to study outflows (notably the hydroxyl molecule), mid- and far-infrared (MIR/FIR) imaging of dust, and resonant-line emission in the rest-frame ultraviolet (UV). In the second category are surveys with integral field spectrographs (IFSs), with multi-object long-slit spectrographs, and with the Cosmic Origins Spectrograph (COS) on the *Hubble Space Telescope (HST)*.

Excellent and thorough reviews from previous decades of theory and observations of GWs provide in-depth discussions of the quantities of observational interest and the astrophysics of GWs (e.g., [1,2]). They also show the trajectory and progress of the field. The scope of this review is narrower. I synthesize observational results from the current decade (approximately 2010 through the present). I focus on direct measures of outflows and do not discuss studies that infer the presence or properties of GWs by studying other phenomena.

As an example of an indirect measurement of the presence or properties of GWs, studies of the mass-metallicity relation constrain how efficiently GWs eject metals from galaxy disks compared to metal production and reaccretion (e.g., [3]). A second example is the significant reservoirs of highly ionized carbon and oxygen that preferentially arise in the circumgalactic media of actively star-forming galaxies [4–8]. A logical source of these metals is stellar GWs. Third, the hot halos that appear to be a common feature of star-forming galaxies [9] may be produced by stellar GWs. Finally, cosmological simulations typically use numerical prescriptions for the unresolved physics of stellar GWs and compare simulated galaxy properties with observed galaxy properties (like the galaxy mass function) to constrain the nature of GWs (e.g., [10–12]). Such indirect measurements are essential for a complete picture of the relationship of GWs to their surrounding environments. However, at present, interpretations of these measurements based on stellar GWs typically compete with other physical models and are rarely definitive.

Stellar processes are not the only possible drivers of GWs. Evidence continues to accumulate that actively accreting supermassive black holes (active galactic nuclei, or AGN) are also important in powering GWs in galaxies with above-average masses (see reviews in [13,14]). However, it can be difficult to distinguish whether the AGN is energetically important for the GW if significant star formation is also present, except in the most powerful AGN. This difficulty is due to the possible power sources being cospatial at low resolution and to the uncertain duty cycle of AGN. Consequently, in this review I focus on studies of purely star-forming systems, or at least those where star formation clearly dominates the galaxy's luminosity. AGN with low-to-moderate Eddington ratios are almost certainly present in many galaxies classified as purely star-forming [15,16], but their energetic importance for GWs remains unquantified.

I organized this review at the highest level by redshift. This is useful for two reasons. First, star formation and galaxy properties at redshifts above unity differ significantly from those in the local universe. The global star formation rate (SFR) peaked at $z \sim 1.9$ (e.g., [17]) and gas mass fraction increases with increasing redshift (e.g., [18]). Galaxies may grow from the inside out, meaning that disks are more extended compared to stars at high z [19,20]. Second, low-z winds are much better characterized because many more techniques can be brought to bear. Some techniques are in practice easier to apply to high-redshift galaxies, but on balance this is not the case.

2. Winds Driven by Star Formation at Low redshift

Most data on nearby stellar GWs in the first 20 years of earnest work came from the optical and X-ray bands. These studies fell largely into two classes: (1) long-slit spectroscopic and/or narrowband imaging surveys (e.g., [21–23]) or (2) case studies using optical 3D spectroscopy, X-ray imaging spectroscopy, or narrowband imaging (e.g., [24–27]). This work was primarily focused on starburst galaxies, which lie above the star-forming main sequence in SFR. High-mass starbursts are typically luminous in the infrared (IR) and classified as either luminous or ultraluminous infrared galaxies. These LIRGs and ULIRGs are defined to have $L_{\rm IR} > 10^{11}\ L_\odot$ and $L_{\rm IR} > 10^{12}\ L_\odot$, which corresponds to SFR $> 10\ {\rm M}_\odot\ {\rm yr}^{-1}$ and SFR $> 100\ {\rm M}_\odot\ {\rm yr}^{-1}$ if all the IR luminosity is powered by star formation. Low-mass (dwarf) starbursts are luminous in the UV and optical bands.

New observing capabilities, surveys, and archival databases have allowed probes of more physical conditions, broadening the picture of winds sketched first by small studies of the warm and hot ionized and cool neutral phases. They have also extended the study of winds to main-sequence galaxies.

This section is divided into four parts. First, I discuss new UV surveys of nearby starbursts. Second, I visit the use of the Sloan Digital Sky Survey (SDSS) for outflow studies. Third, I summarize results from the widening use of integral field spectroscopy. I end by surveying significant advances in revealing and quantifying the molecular gas and dust in GWs using ground-based submillimeter and space-based FIR telescopes.

2.1. Ultraviolet Surveys

The rest-frame UV contains many interstellar absorption lines and Lyα, the brightest UV emission line in unobscured starbursts. Previous UV instruments have been used to study individual systems or small samples, but the sensitivity of COS has enabled population studies of low-z, UV-bright starbursts at high signal-to-noise (S/N). These studies are large enough to study correlations between the properties of GWs and galaxy properties.

Two studies find a correlation between the velocity of the ionized outflow and basic properties of the galaxy and starburst itself: stellar mass M_* and star formation rate SFR [28,29]. Table 1 compares these correlations and the ionization states probed. The first [28] uses COS data on 48 starbursts at $z < 0.26$ taken from the literature. The second [29] combines COS and *Far-Ultraviolet Spectroscopic Explorer (FUSE)* data on 39 starbursts at $z < 0.25$ [30] plus MMT or Keck spectra of 9 compact starbursts at $z = 0.4 - 0.7$ [31,32]. Notably, the studies differ in their definition of outflow velocity. The first [28] uses the 50% and 90% points in the cumulative velocity distribution (CVD; starting from the red side of the line). The second [29] uses either the 98% point of the CVD (in the case of data taken from secondary sources [31,32]) or the authors' own velocity measurements ($v_{\rm max}$). I label the correlations from this second study with $v_{\rm max}$ for simplicity.

Table 1. Log-Log Fits of Outflow vs. Galaxy Properties.

Axes	Tracer	IP (eV)	N	Range	Slope	p	Reference
$v_{50\%}$ vs. SFR	Si II	16.3	48	$10^{-1} - 10^{2}$ M$_\odot$ yr^{-1}	0.22 ± 0.04	<0.001	[28]
$v_{50\%}$ vs. SFR	Na I	5.1	41	$10^{-1} - 10^{3}$ M$_\odot$ yr^{-1}	0.35 ± 0.06	···	[33]
$v_{50\%}$ vs. SFR	Na I	5.1	13	$10^{0.8} - 10^{2.2}$ M$_\odot$ yr^{-1}	0.15 ± 0.06 [c]	···	[34]
$v_{50\%}$ vs. SFR	Na I	5.1	13	$10^{0.8} - 10^{2.2}$ M$_\odot$ yr^{-1}	0.30 ± 0.05 [c]	···	[34]
$v_{90\%}$ vs. SFR	Si II	16.3	48	$10^{-1} - 10^{2}$ M$_\odot$ yr^{-1}	0.08 ± 0.02	0.002	[28]
$v_{90\%}$ vs. SFR	Na I	5.1	59	$10^{-1} - 10^{3}$ M$_\odot$ yr^{-1}	0.21 ± 0.04	<0.001	[23]
$v_{90\%}$ vs. SFR	H I, N II	13.6–29.6	48	$10^{0.7} - 10^{2.6}$ M$_\odot$ yr^{-1}	0.24 ± 0.05	<0.001	[35]
$v_{\rm max}$ vs. SFR	Si II, C II, Mg II	15.0–24.4	48	$10^{-2} - 10^{3}$ M$_\odot$ yr^{-1}	0.32 ± 0.02	<0.0001	[29]
$v_{50\%}$ vs. M_*	Si II	16.3	48	$10^{9} - 10^{11.5}$ $M_\odot$	0.20 ± 0.05	0.002	[28]
$v_{90\%}$ vs. M_*	Si II	16.3	48	$10^{9} - 10^{11.5}$ $M_\odot$	0.12 ± 0.03	0.003	[28]
$v_{90\%}$ vs. M_* [b]	Na I	5.1	52	···	0.28 ± 0.08	<0.001	[23]
$v_{50\%}$ vs. $v_{\rm circ}$ [a]	Si II	16.3	48	$10^{1.8} - 10^{2.5}$ km s^{-1}	0.87 ± 0.17	0.002	[28]
$v_{90\%}$ vs. $v_{\rm circ}$	Na I	5.1	20	$10^{1.4} - 10^{2.7}$ km s^{-1}	0.85 ± 0.15	<0.001	[23]
$v_{90\%}$ vs. $v_{\rm circ}$ [a]	Si II	16.3	48	$10^{1.8} - 10^{2.5}$ km s^{-1}	0.44 ± 0.09	0.003	[28]
$v_{\rm max}$ vs. $v_{\rm circ}$ [a]	Si II, C II, Mg II	15.0–24.4	48	$10^{1.3} - 10^{2.5}$ km s^{-1}	1.16 ± 0.37	<0.0001	[29]
η vs. M_*	O I, Si II–Si IV	13.6–45.1	7	$10^{7} - 10^{11}$ $M_\odot$	-0.43 ± 0.07	<0.001	[36]
η vs. M_*	H I, N II	13.6–29.6	33	$10^{9.6} - 10^{11.2}$ $M_\odot$	-0.43	···	[35]
η vs. M_* [b]	Na I	5.1	42	$10^{10} - 10^{11}$ $M_\odot$	-0.95 ± 0.20	0.006	[23]
η vs. $v_{\rm circ}$ [a]	O I, Si II–Si IV	13.6–45.1	7	···	-1.56 ± 0.25	<0.001	[36]

IP gives the ionization potential range of the atomic tracers; N is the number of galaxies in the fit; the range applies to the galaxy property in the fit; the slope is for a linear fit in log-log space (or the exponent of a power law fit in linear space); and the p-value is the estimated likelihood of a null correlation. For references where only the correlation coefficient is provided, the p-value is inferred from it. [a] $v_{\rm circ}$ is calculated from M_* using a linear scaling. [28,36] use $\log(v_{\rm circ}/{\rm km\ s^{-1}}) = 0.28 \log(M_*/M_\odot) - 0.67$ from [37], while [29] uses $\log(v_{\rm circ}/{\rm km\ s^{-1}}) = 0.29 \log(M_*/M_\odot) - 0.79$. [b] M_* is assumed to be proportional to the K-band luminosity. [c] The first of these fits uses integrated spectra; the second is from spatially resolved fits.

While both studies find correlations, the ranges of galaxy properties in one are wider [29]. This study also finds steeper slopes in lines fitted to the data; the slopes from the two studies differ at $> 1\sigma$. The second study does not specify a fitting method [29] , while the first uses a method that accounts for x and y errors, outliers, and scatter [28]. Neither study finds a significant correlation between outflow velocity and specific star formation rate sSFR $\equiv$ SFR/M_*. One also finds no correlation with star formation rate surface density $\Sigma_{\rm SFR}$, but their sample has a range $\Sigma_{\rm SFR} = 10^{-2} - 10^{1}$ M$_\odot$ yr^{-1} kpc^{-2} [28]. The second study adds three orders of magnitude to the upper end of this range and do find a correlation, which they parameterize as $v_{\rm max} = 3296/[(\Sigma_{\rm SFR}/1307.9)^{-0.34} + (\Sigma_{\rm SFR}/1307.9)^{0.15}]$ at a significance of $p < 0.0001$ [29].

The mass outflow rate $\dot{M}$ and mass outflow rate normalized to the star formation rate ($\eta \equiv \dot{M}/\mathrm{SFR}$)[1] were computed for subsamples of these two larger samples [30,36]. One study estimates the wind column density using multiple ions and a stacked spectrum; they apply this single column density to the entire sample of 39 galaxies [30]. Their mass outflow rate is then a product of the outflow velocity and starburst radius times a constant. They find a correlation between $\dot{M}$ and SFR that is near-linear (though the slope is unquantified) and which appears to be driven largely by the correlation between $\dot{M}$ and v_{max}. They also find that η is inversely correlated with SFR and M_* (or v_{circ}).

The other study finds a similar result for the inverse correlation of η and galaxy mass ([36]; Figure 1; Table 1). While based on a much smaller sample size, this work uses high signal-to-noise spectra, velocity-resolved optical depths and covering factors, and photoionization modeling to estimate the ionization state, density, metallicity, and inner radius of the wind (assuming a model relating velocity and radius). The measured slope (-0.43 ± 0.07) matches predictions from numerical simulations, which are in the range -0.35 to -0.50 at low masses [38,39,41,42].

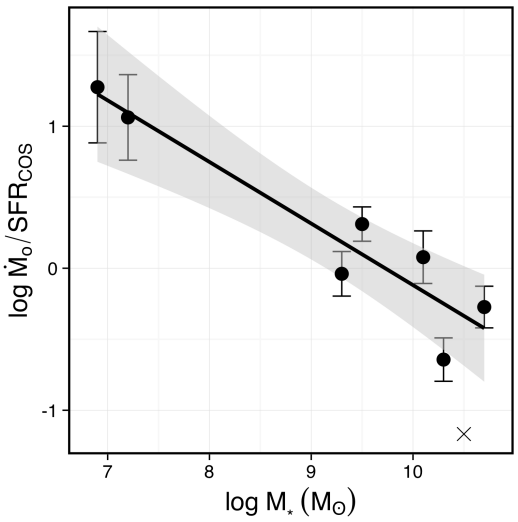


Figure 1. A fit to $\eta \equiv \dot{M}/\mathrm{SFR}$ vs. M_* for a sample of nearby GWs [36]. The gray region is the 95% confidence interval. Outflow masses have been estimated from multiple rest-frame UV absorption lines and photoionization modeling. Relationships between outflow and galaxy properties are key tools for connecting observations to theory. The fitted slope of -0.43 ± 0.07 compares favorably with predictions from numerical simulations at low masses [38,39,41,42]. At higher masses the slope may be steeper, as suggested by some simulations [39,42] and measurements [23]. Reproduced with permission from Figure 1 of reference [36].

The velocity measurements in these UV surveys employ lines from ions of relatively low ionization potential [28,29], while the estimated wind masses are inferred from a larger range of ions [30,36]. The resulting fits to GW vs. galaxy properties are in overall agreement with similar fits made a decade earlier using the cool, neutral gas phase (Table 1; [23,33]). The spread in fitted slopes illustrates the systematic uncertainties in this enterprise, but a conservative synthesis points to velocity depending on SFR and M_* as $v \sim \mathrm{SFR}^{0.1-0.3}$ and $v \sim M_*^{0.1-0.3}$. The dependence on circular velocity is thus

[1] This quantity has an uncertain physical interpretation, though at face value it might quantify the capability of a wind to act as negative feedback on star formation. The logic is: if $\eta > 1$, then more gas is leaving the region than is forming stars. Thus, the outflow is going to deplete gas more quickly than star formation (maybe leading to fewer stars in the end). It is sometimes referred to as the mass-loading efficiency or factor, perhaps suggesting that it measures the amount of gas that is "loaded" into the wind as it moves through the galaxy. That is, it is the ratio of the mass of gas that eventually emerges from star-forming regions to the mass of outflowing gas that is initially produced by star formation through, e.g., stellar winds and supernovae. However, it is not a direct measure of this. The term mass-loading originated with studies of how much cool, ambient gas is mixed into a hot wind phase in the model of a wind driven by a hot fluid.

steeper (close to linear). The upper end of the range of slopes of v vs. SFR matches a prediction from simulated absorption lines in 3D hydrodynamic simulations [40]. There are fewer measurements of how η depends on various properties, and the systematic uncertainties in η are higher than in velocity. However, as discussed above, published fits are surprisingly consistent with predictions from numerical simulations [41,42], including at high masses where the slope steepens [23,42].

This begs the question of what drives the scatter in these relationships. It is worth noting that the pursuit of scaling relations relies on reducing the velocity field of a galactic outflow to a single parameter in a single tracer. Outflows are unlike galaxies in that they are inherently a violent, non-equilibrium process whose structural properties are governed by time-varying power sources, gas hydrodynamics, and radiation transfer rather than gravitational processes. Their properties thus almost certainly depend on multiple host parameters simultaneously. The fact that outflow properties scale at all with bulk galaxy properties such as SFR is not surprising (more energy means higher-velocity gas). There are clearly important details beyond this, however, that are harder to quantify and may reflect the unique structural properties or history of particular galaxies (Is it a merger? Did the outflow just turn on?) or other hidden scalings that are orthogonal to those with SFR and mass. One solution might be to combine multiple galaxy or wind properties into single parameters in search of an "outflow fundamental plane," but combining, e.g., two parameters into one has yet to noticeably improve matters [29,36].

The imprint of GWs in the UV is found not only absorption lines but also in Ly emission lines and the escape of ionizing radiation beyond the Lyman limit. Extended Lyα emission and Lyman continuum (LyC) escape may be caused in part by outflows that create low-density holes in a galaxy's ISM.

Recent studies of Lyα and absorption lines in samples of order tens of galaxies have quantified the impact of outflows on the properties of Lyα and the escape of LyC. Population studies of Lyα in nearby galaxies are, however, more complicated to interpret than studies of absorption lines because of the resonant emission and absorption behavior of Lyα and its sensitivity to dust. As a result, these studies have not reached firm conclusions on how these tracers reflect GW properties. There is some suggestion that outflow velocity is correlated with Lyα escape fraction [43–49]. However, this correlation has significant scatter, and cases exist of low outflow velocity and high LyC escape [49]. Lyα and outflow velocity are also both correlated with SFR and/or $\Sigma_{\rm SFR}$ [47,48]. In one sample, galaxies with and without escaping LyC have similar outflow velocities [48]. The simple presence of outflows may be a necessary but not a sufficient condition for Lyα and/or LyC escape [45]; other factors such as the outflow acceleration, low H I column density, or low metallicity may also be required for Lyα or LyC to exit the dense regions of a galaxy [44,46,48].

2.2. Single-Aperture Surveys

Searches for outflows in single-aperture optical spectroscopic surveys like SDSS are hampered by the spatially unresolved bright host galaxy. Outflow features in emission lines are typically overwhelmed by ionized gas emission from the star-forming host disk, which in galaxies with modest GWs lies in the same velocity range as the outflow. Interstellar absorption lines can be similarly dominated by stellar absorption features.

Both limitations can be overcome with data of high enough S/N and high-quality modeling of the underlying stellar continuum. Stacking of many spectra is commonly used to achieve the required S/N, and stellar models that match the spectral resolution of SDSS are mature. (Even if these models may not uniquely constrain the star formation history or stellar population properties, they fit the data very well.)

Three studies of GWs in star-forming galaxies have stacked SDSS DR7 data. The authors of the first of these stack 10^5 high-mass ($M_* \sim 10^{10} - 10^{11}\ M_\odot$) galaxies in bins of various physical parameters to study the properties of cool, neutral outflows using the interstellar Na I D doublet [50]. They detect this resonant line in both absorption and emission. They find that the velocity and equivalent width of absorption scale with inclination, such that face-on galaxies are observed to have

faster, higher equivalent width outflows, consistent with the model of minor-axis outflows. Outflow equivalent width and linewidth also correlate with $\Sigma_{\rm SFR}$ (over the range $10^{-2.5} - 10^{-0.5}$ $M_\odot$ yr^{-1} kpc^{-2}) and M_* (over the small range $10^{10.3} - 10^{11.2}$ $M_\odot$). However, systemic interstellar absorption also scales with $\Sigma_{\rm SFR}$ and M_*, so the nature of these correlations is uncertain.

The second study uses 200,000 galaxies to stack by SFR and M_* over a range of galaxy properties comparable to the ranges in samples of individual galaxies ([51]; Table 1; Sections 2.1 and 2.3): SFR = $10^{-2.7} - 10^{2.3}$ $M_\odot$ yr^{-1} and $M_* = 10^{7.3} - 10^{11.8}$ $M_\odot$. They fit [O III] 5007 Å, Hα, and [N II] 6548, 6583 Å using a high S/N instrumental profile and extract the line-of-sight velocity distribution (LOSVD) of both the ionized gas and stars. They use excess blueshifted emission-line gas at the extreme end of the gas LOSVD to measure outflow velocity, with the stellar LOSVD serving as a reference. For star-forming galaxies selected by line ratio [52], these authors find that $v_{\rm out}$ correlates significantly with SFR and sSFR. $v_{\rm out}$ does not correlate with M_*, though it does with stellar velocity dispersion, suggesting a discrepancy in how these quantities are measured. This method is most sensitive to higher-velocity outflows, and outflows are detected primarily at SFR > 1 $M_\odot$ yr^{-1} and sSFR $> 10^{-9}$ yr^{-1}. They are also preferentially observed in galaxies with SFR values that put them above the main sequence.

Finally, a third study employs a similar technique over a larger sample of 600,000 galaxies in bins of SFR and M_* [53]. These authors apply two methods for parameterizing outflows: (1) they fit the [O III] emission line in each stack using two Gaussians; and (2) they use the observed [O III] profile as the gas LOSVD and calculate measures of line width and asymmetry. They then remove the instrumental resolution in quadrature. They find no significant detection of starburst-driven winds in star-forming galaxies. However, they select star-forming galaxies using a more restrictive line-ratio criterion [54] than the ionized gas study that does detect stellar GWs [51]. They argue that a more permissive selection [52] allows low-luminosity AGN to contaminate a sample of star-forming galaxies; these AGN could in turn produce outflows in galaxies that are supposedly purely star-forming. Low-luminosity AGN exist throughout the star-forming sequence with a range of contributions to [O III] [15,16]. It is certainly plausible that star formation, rather than low-luminosity AGN, powers the outflows detected in galaxies whose line emission is dominated by star formation [51], but separating potential contributions from low-luminosity AGN requires further work.

These stacking studies add weight to the conclusions drawn from studies of smaller samples and individual galaxies by probing more statistically complete samples of galaxies across a wider range of basic galaxy properties. There is agreement between two of the stacking studies discussed above that ionized and/or neutral winds are a common feature of galaxies of modest to high SFR across the mass spectrum [50,51], consistent with results discussed elsewhere in this review. The disagreement with the third study [53] on this point is puzzling, though the difficulty of separating AGN from star formation as a possible energy source in galaxies with supermassive black holes accreting at lower Eddington ratios is a valid concern. Furthermore, the correlations between wind and galaxy properties are akin to those seen using UV and other optical studies (Section 2.1; Table 1), and the connection to inclination angle is consistent with a wide range of observational results.

2.3. IFS Results

Though they cannot yet match the numbers of galaxies observed in the SDSS, spatially resolved spectroscopic surveys with optical IFSs promise to significantly improve the detectability and characterization of GWs. This is true both at ground-based resolution and with enhanced spatial resolution from adaptive optics; the latter is important for probing the nuclear regions of galaxies where GWs emerge from their power sources. Studies of one or a few galaxies with stellar GWs published in the current decade are numerous [55–64]. These detailed case studies highlight the ubiquity and complex, multiphase nature (ionized, neutral, dusty) of these winds (Figure 2) and the power of IFS for leveraging the combination of spectral and spatial information to separate outflows from their hosts.

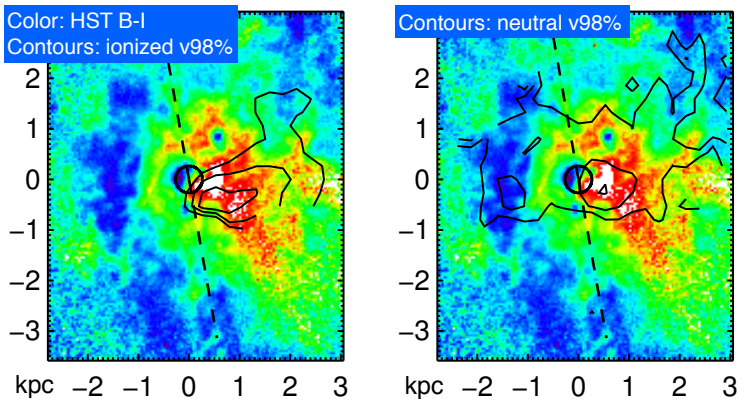


Figure 2. Illustration of the complex, multiphase structure of a nearby starburst-driven GW as observed with IFS (F10565+2448; [57]). The background color maps are *HST* images of $F435W - F814W$ (or $B - I$), where red and white indicate the reddest colors. They show dusty filaments emerging from the obscured starburst along the minor axis in red and white; the near side of the star-forming disk is shown as the blue clumpy regions to the left in each panel. The galaxy major axis is the dashed line, and the contours show ionized gas $v_{98\%}$ on the left (-800, -700, -600 km s^{-1}) and cool, neutral $v_{98\%}$ on the right (-700, -600, -500 km s^{-1}). The minor-axis outflow reveals dusty filaments and unresolved gas motions of hundreds of km s^{-1}, consistent with a shocked outflow with layered clumps of gas. The axes are in kpc. Reproduced by permission of the AAS from Figure 17 of reference [57].

Small surveys using instruments that target one galaxy at a time have characterized GWs in galaxies with the highest star formation rates. The authors of a study of the ionized gas in 27 LIRGs [65,66] found frequent shock ionization accompanied by high gas velocity dispersions, a conclusion supported by an earlier long-slit study of ULIRGs [67]. The line ratios are consistent with models of slow shocks, correlate with $\sigma_{\rm gas}$, and may be caused in part by GWs [65,66].

The authors of a larger study of the ionized and cool, neutral gas in ∼50 LIRGs and ULIRGs [34,35] concur that high ionized gas linewidths are shock-powered. To detect GWs, they spatially integrated their spectra [34,35] and/or fit the spatially resolved data [34]. In the former case, they corrected the velocity of each spatial position for gravitational motions and then summed over the field of view. Fits to the wind velocity vs. SFR give best-fit slopes of 0.24 ± 0.05 (ionized gas), 0.15 ± 0.06 (integrated neutral gas), and 0.30 ± 0.05 (spatially resolved neutral gas). These are consistent with the single-aperture fits discussed above (Section 2.1; Table 1). η is between 0.1 and 1 in the neutral and ionized gas, with average values similar to those previously estimated in LIRGs and ULIRGs [23,57]. The study of integrated spectra [35] finds evidence that η decreases with increasing dynamical mass over the range $10^{9.6} - 10^{11.2}$ $M_\odot$, with a log-log slope of -0.43 that is identical to that found in the UV over a much wider mass range ([36]; Section 2.1; Table 1). (A steeper slope in this relationship at high masses, as previously measured [23], is predicted by some simulations [39,42].) Finally, these authors fit a relationship between η and $\Sigma_{\rm SFR}$ with a log-log slope of 0.17 [35].

Two major (of order thousands of galaxies) IFS surveys have been ongoing for several years: the SAMI (Sydney-Australian-Astronomical-Observatory Multi-object Integral-Field Spectrograph) Galaxy Survey [68] and MaNGa (Mapping Nearby Galaxies at Apache Point Observatory) [69]. These surveys employ instruments that target multiple galaxies at once, each with a single, small IFS. Though limited in spatial resolution (of order $2''$), the ability of these surveys to integrate to high S/N, collect large samples of galaxies across a wide parameter range, and separate the outflow from the host galaxy using both spatial and spectral information with IFS promises more accurate statements about the ubiquity and property of stellar GWs over a wider range of galaxy types.

The first result from these surveys relies on a sample of 40 edge-on SAMI disk galaxies [70]. These authors use minor-axis kinematic asymmetries to detect winds and find them down to very low $\Sigma_{\rm SFR}$ (10^{-3} M$_\odot$ yr^{-1} kpc^{-2}). The asymmetry increases with $\Sigma_{\rm SFR}$ and is associated with recent bursts of

star formation. The connection of the asymmetry to GWs and its association with high Σ_{SFR} and high-temperature extraplanar gas is bolstered by comparison to simulations [71].

2.4. Molecular Gas and Dust

The most rapid progress in the study of stellar GWs has come from molecular gas and dust continuum measurements. The direct dust measurements have been made in the MIR/FIR using space-based telescopes: *AKARI*, the *Spitzer Space Telescope*, and the *Herschel Space Observatory*. The molecular gas measurements have been led by ground-based interferometers such as the Atacama Large Millimeter/submillimeter Array (ALMA), SubMillimeter Array (SMA), Institut de Radioastronomie Millimétrique (IRAM) Plateau de Bure interferometer (PdBI), and Nobeyama Millimeter Array (NMA), though *Herschel* has also played an important role. While sample sizes are still small and most studies have focused on individual galaxies in the starburst regime, results point to the ubiquity of dusty molecular gas entrained in stellar GWs.

Recent interferometric measurements of CO transitions have uncovered outflowing cold molecular gas in approximately 11 nearby LIRGs and ULIRGs whose energy output is dominated by star formation [72–79]. Molecular outflows in four very nearby star-forming galaxies with lower SFR have also been studied in detail: NGC 3628, M82, NGC 253 (Figure 3), and NGC 1808 [80–83]. M82 had been the only previous starburst galaxy known to host a molecular outflow [84,85].

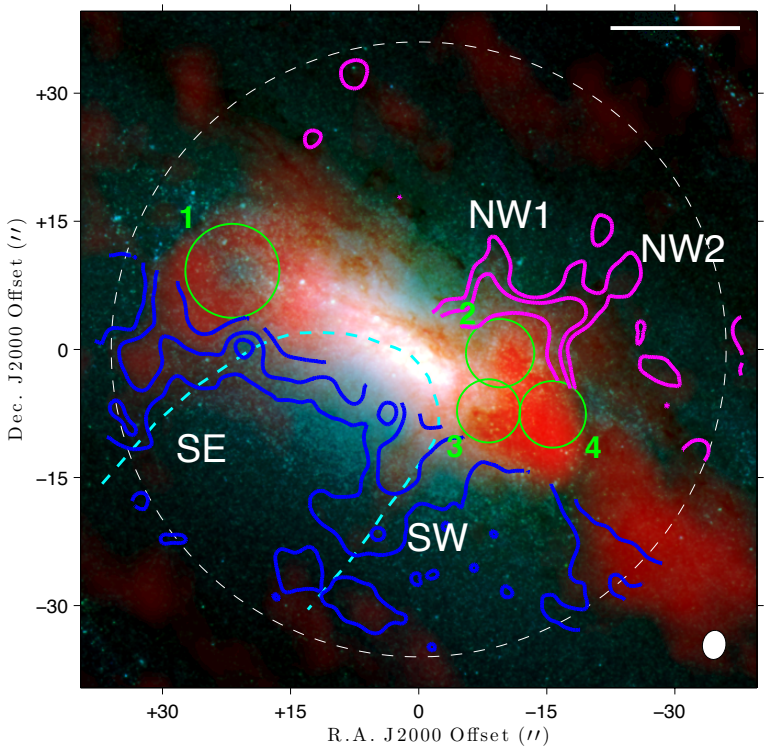


Figure 3. One of the nearest and best-resolved molecular gas outflows in NGC 253 [81]. The background image is *HST* NIR (blue+green) and ALMA CO (red). The blue (magenta) contours show the approaching (receding) CO outflow. The green circles outline expanding molecular shells. The white bar is 250 pc long. The dashed cyan contour outlines the warm/hot ionized outflow that is interior to the molecular gas streamers and extends to larger scales (Section 2.4; [86]). NGC 253 is one of only a few examples of the characteristic minor-axis filaments of a GW in molecular gas and their relationship to the disk and other gas phases. Reprinted by permission from reference [81], ©2013.

These molecular outflows are typically confined to the inner kpc of the galaxy (in radius). They have modest outflow velocities in nearby disks (tens to a few hundred km s^{-1}) but have a broader range of peak velocities in the more luminous starbursting disks and mergers (300–800 km s^{-1}). Similarly,

the outflow rates appear to scale with SFR and/or Σ_{SFR}. The nearby, low-luminosity starbursts have $\dot{M}$ values of a few to a few tens of $M_\odot$ yr^{-1}, while the LIRGs and ULIRGs have a broader range of estimated $\dot{M}$: several to several hundred $M_\odot$ yr^{-1} (perhaps even $\sim$1000 $M_\odot$ yr^{-1} in F17208−0014; [75]). Mass outflow rates of these magnitudes are similar to the star formation rates in these systems, and equal to or larger than the mass outflow rates estimated in other gas phases. The larger mass outflow rates in the molecular phase are due primarily to larger total outflowing gas masses.

Dense gas, as probed by characteristic molecules such as HCN and HCO^+, is also a common feature of these outflows. It is present in the extended outflows of M82, NGC 253, NGC 1808, and Arp 220, as observed in emission using interferometry [78,87–90]. Outflowing dense molecular gas has also been observed in absorption in the inner regions of the highly obscured binary Arp 220 [91–94].

The ubiquity of starburst-driven molecular outflows was first discovered using FIR OH and H_2O absorption lines with *Herschel* [95–99]. The outflow properties inferred from these spatially unresolved absorption lines and detailed radiation transfer models are comparable to measurements from molecular emission-line interferometry [99]: massive, high-velocity but compact flows.

The cold molecular and cool atomic gas share similar dynamics. Global OH properties correlate with those measured from the 158 μm [C II] emission line [100], which traces photo-dissociation regions (PDRs). The 158 μm [C II] line may be a key technique for tracing outflows at high z as it moves into the submillimeter band. OH properties may also correlate with Na I D atomic gas measurements [23,33,57,98–101], though there is significant scatter in this correlation. On the spatially resolved level, FIR atomic fine structure lines are seen in the GWs of M82 [102], NGC 2146 [103], and NGC 253 [104]. In M82 and NGC 253 these atomic PDR tracers correlate well with the molecular gas in terms of morphology and dynamics [102,104].

Direct observations of atomic H I in outflows may become possible with the next generation of sensitive radio arrays. New Jansky Very Large Array H I data on M82 are consistent with a deceleration of the outflow as it moves upward into the halo [105], suggestive of a galactic fountain [82].

Warm molecular gas does not contribute significantly to the mass budget of outflows, but the strength of its emission lines in the accessible NIR band makes it a useful tracer of the extent and physical state of molecular gas. Deep near-infrared (NIR) imaging and spectroscopy shows that shocked, warm H_2 in the M82 outflow extends several kpc from the disk along the minor axis [106,107]. Outflowing warm molecular gas has been detected in several nearby, starburst-dominated ULIRGs using the 2.12 μm H_2 1-0 S(1) transition [60,108,109]. These outflows are compact (<2 kpc), with velocities of a few hundred km s^{-1}, and the relationship between the cold and warm phases requires further study. Indirect evidence from the global properties of a large sample of ULIRGs implicates shocks in GWs as the origin of excess warm H_2 in this population [110].

Dust and molecular gas are abundant under similar physical conditions. Observations of filamentary dust structures along disk minor axes in some wind systems and the correlation of these dust features with outflowing atomic gas columns are indirect evidence for outflowing dust in stellar GWs (Figure 2; e.g., [50,57,111]). Further evidence in the form of UV reflection nebula and polarized line emission strongly suggests the presence of dusty winds in M82 and NGC 253 [112–114]. Modeling of UV reflection in the M82 wind indicates smaller average grain sizes in the M82 wind compared to the disk [114,115].

Observations of thermal emission from dust in galaxies where the disk and outflow can be spatially separated strengthen the case that stellar GWs are dusty in at least some cases. Studies detect 1–4$\times10^6$ $M_\odot$ of dust in M82 (traced at 7–500 μm) extending far from the disk plane [116,117], as well as significant amounts of cold dust emplaced by tidal interaction with M81 [118].

Roughly 10^6 $M_\odot$ of warmer dust (traced at 70–160 μm) is also found in the outflows of NGC 253 and NGC 4136 [119,120] in structures that correlate with ionized gas emission at other wavelengths. The extended cold dust in NGC 4631, however, may be of tidal origin [120], as in the case of M82. In the dwarf galaxy NGC 1569, 70–500 μm imaging indicates a large reservoir (a few times 10^5 $M_\odot$) of circumgalactic dust, perhaps deposited by its starburst-driven GW [121]. At shorter

wavelengths, GW features in NGC 1569 are seen in warm dust emission [122]. Contrary to these results, no dust is detected at 37μm in the NGC 2146 wind [103]. FIR observations of dwarf galaxies with outflows observed at other wavelengths paint a nuanced picture of dusty outflows in systems with lower SFR [121]; few systems show abundant circumgalactic dust or strong correlations with multiwavelength signatures of GWs.

Finally, polycyclic aromatic hydrocarbons (PAHs) are prominent features of GWs in those galaxies in which they have been detected. As alternately large molecules or small dust grains, PAHs bridge the gap between molecular gas and dust and are luminous features in rest-frame 3–20 μm spectra. An enormous PAH nebula extends from the M82 disk [123] and shows evidence for grain shattering from PAH line ratios [107,124]. PAHs have been found in GWs in other galaxies [125,126], and the amount of extraplanar PAH emission in galaxies may correlate with $\Sigma_{\rm SFR}$ [126].

The warm and hot ionized gas traced by UV absorption lines, optical emission lines, and X-rays are prevalent in GWs (Sections 2.1– 2.3). Quantifying the physical relationship between the molecular and ionized gas phases thus appears to be within reach. In a few nearby systems this connection has been made, but there has been no attempt for most galaxies (probably because the ability to detect the molecular phase of the outflow is still relatively new). There is a need for sensitive, multiphase studies at the highest spatial and spectral resolution to connect these outflow components.

M82 and NGC 253 both have deep, high-spatial-resolution maps of warm ionized gas (Hα), hot ionized gas (soft and hard X-rays), and molecular gas. These two exemplars paint a picture of an innermost hot, ionized wind fluid [27] that entrains warm and hot ionized material which are spatially correlated with each other and surround the hot fluid, perhaps as a shell [86,127]. The cold molecular gas in turn envelops these ionized phases as it is entrained from the disk (Figure 3; [81,82]). The relationship between the warm molecular and ionized phases, however, is likely more complex. In examples of minor-axis outflows where both are spatially resolved, there is coarse-grained spatial correlation (Arp 220 [78,128], F08572+3915 [57,129], and M82 [106]), but in other cases there is not (NGC 4945; [130]). At very high spatial resolution, apparent correlation may break down [106]. Note that the outflows in some of these galaxies may be AGN-driven, but they are included here because the sample size of galaxies with resolved molecular and ionized outflows is unfortunately small.

3. The Nearest Galactic Wind

The unexpected recent discovery of the so-called Fermi bubbles–large, diffuse γ-ray structures that form a bipolar shape above and below the Galactic plane–has revived interest in characterizing the GW in the Milky Way [131,132]. Previous data provided strong evidence of its existence (see references in [2]), but the picture-perfect morphology of the Fermi bubbles make it an almost inarguable fact.

This review is concerned with observations of starburst-driven GWs, and the Milky Way's GW may be driven by star formation (e.g., [133]). It also may be powered by the Galactic nuclear black hole during a previous accretion episode (see, e.g., the recent review of relevant data and models in [134]). However, for completeness we note some recent observations, since the Milky Way is an excellent laboratory for studying a GW at high sensitivity and spatial resolution in what is a "typical" galaxy in the Local Universe. Since its discovery, the Fermi bubbles have notably been found to also contain a magnetized radio plasma [135] and have been connected to the previously known microwave "haze" that was re-observed with *Planck* [136]. The bubbles also appear to host neutral gas clouds moving up to several hundred km s^{-1} [137–139], as well as higher-ionization species observed in absorption [140–143]. These neutral and ionized clouds may lie along filaments swept up by the bubble along its edges, though their contribution to the structure and mass/energy budget of the outflow are not yet clear.

A recent claim has also been made for a GW in a satellite of the Milky Way. This potential outflow in the Large Magellanic Cloud was extrapolated from absorption-line measurements of a single line of sight through its disk [144]. The LMC contains 30 Doradus, which is undergoing a significant star formation episode.

4. Winds Driven by Star Formation at High redshift

The presence and ubiquity of stellar GWs outside of the local universe was first evident in blueshifted rest-frame UV absorption lines and complex Lyα profiles in Lyman-break galaxies (LBGs) (e.g., [145–147]). Information on stellar GWs at high z comes predominantly from single-aperture, down-the-barrel spectroscopy of rest-frame UV lines. ("Down-the-barrel" refers to sightlines toward the galaxy itself.) However, newer instruments and techniques have in the past decade opened other avenues to study high z winds. These include rest-frame optical measurements of emission lines with wide-field, NIR, multi-object spectrographs; multiplexed or wide-field IFS instruments such as the K-band Multi-Object Spectrograph (KMOS) and the Multi-Unit Spectroscopic Explorer (MUSE) that enable multi-object and/or spatially resolved measurements; NIR, adaptive optics IFS to achieve high spatial resolution; FIR and submillimeter observations that probe molecular and atomic gas transitions; and transverse-sightline spectroscopic surveys. These new techniques have established the ubiquity and properties of stellar GWs in new galaxy populations and constrained the redshift evolution of their bulk properties.

Deep spectroscopy of strong rest-frame optical emission lines (mainly Hα and [N II]) at $z \sim 2$ reveals broad wings that arise primarily from bright star-forming regions [148–151]. These broad wings, which appear to extend over several kpc and strengthen with increasing $\Sigma_{\rm SFR}$, have been interpreted as evidence of stellar feedback. Similar wings are found in massive, compact star-forming galaxies over a wider wavelength range [152].

Larger spectroscopic surveys (up to ∼500 galaxies) of star-forming galaxies at $z = 0.3 - 2$ use the low-ionization metal lines Mg I, Mg II, and Fe II to probe GWs [154–163]. Resonant transitions from outflows in absorption (blueshifted) and emission (redshifted), as well as corresponding non-resonant transitions, constrain basic outflow properties such as velocity and ionization state and, potentially, more complex structural parameters (Figure 4; [164]). These high-z, low-ionization outflows are broadly consistent with those found at low z: they have modest velocities (up to a few hundred km s^{-1} on average); their properties (velocity and equivalent width) correlate with SFR, $\Sigma_{\rm SFR}$, and M_*; their detection rates in absorption average a few tens of percent, indicative primarily of the wind geometry (a high frequency of occurrence of non-spherical winds); they have estimated mass-loss rates of order the star formation rate, though with considerable uncertainty; and they are preferentially found in face-on galaxies (or their properties are more extreme in face-on galaxies), consistent with minor-axis flows. The velocities of these winds may increase with increasing z for galaxies of given SFR, possibly due to increasing star formation rate surface density [158,165–167], and with increasing ionization potential [167–169]. Extended, scattered emission (both resonant and non-resonant) from low-ionization species has been probed in detail in a handful of systems [153,170–172] and is now recognized as a common feature of star-forming galaxies at these epochs [163,173,174]. Pure resonant emission is seen at low SFR, transitioning to P-Cygni or pure-absorption resonant profiles plus non-resonant emission at high SFR, indicative of an increasing signature of outflowing gas [163]. In a handful of gravitationally lensed systems, absorption-line analyses of more ions indicate α enhancement and more robustly constrain mass-loss rates [175,176].

At moderate redshifts ($z \sim 0.7 - 0.8$), the presence of low-velocity GWs in poststarburst galaxies points to the possibility that these winds help to quench star formation [173]. Very high-velocity winds (1000 km s^{-1}) found in bluer, rarer post-starbursts [177] appear to be driven by very compact starbursts rather than AGN activity [31,178].

The down-the-barrel technique, which probes low-ionization outflows that emerge along the line-of-sight toward the galaxy disk, is complemented by transverse sightlines through galaxy halos toward background quasars or galaxies. LBGs at $z = 2 - 3$ host both low- and high-ionization gas out to radii ∼100 kpc; because this gas is outflowing over a large solid angle (as inferred from down-the-barrel observations), it is plausibly doing so at large radii [147]. In other samples, Mg II and O VI absorbers show a preference for alignment with galaxy major or minor axes, and the minor-axis gas is preferentially found in blue galaxies. This absorber alignment is suggestive of major-axis inflow

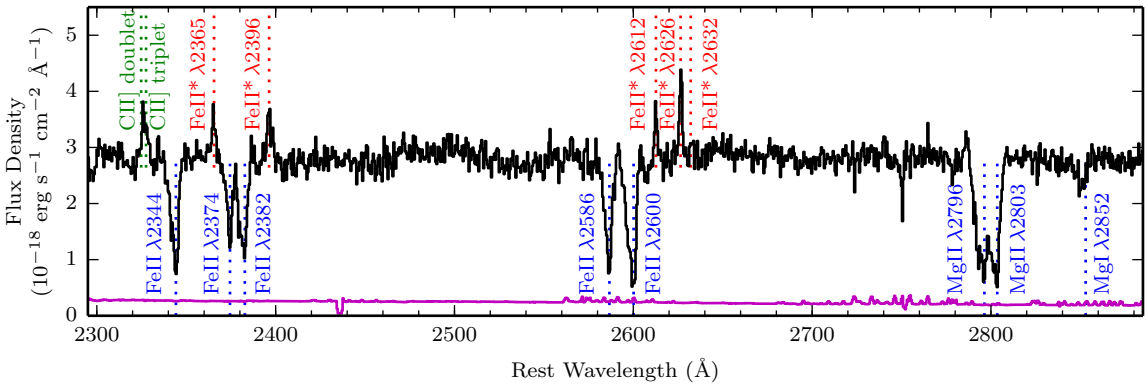


Figure 4. Absorption and emission lines in the outflow of a $z = 1.3$ star-forming galaxy [153]. The resonant absorption lines (labeled in blue) are blueshifted and trace the approaching near side of the outflow. The non-resonant iron emission lines (labeled in red), which are spatially extended along the minor axis, trace the bulk of the outflow. These resonant and non-resonant lines are powerful probes of the presence and properties of high-redshift outflows. Reproduced with permission from Figure 1 of reference [153], ©ESO.

and minor-axis outflow, and the connection to blue galaxies points to star formation as the power source [179,180]. Simple geometric outflow models of halo absorbers yield outflow properties that are consistent with those seen at low z [181–183].

The prominence of Lyα in the spectra of high z galaxies makes it a tempting target for parameterizing outflows (e.g., [184]). However, as mentioned above (Section 2.1), radiation transfer effects make it an ambiguous indicator. Redshifted Lyα does typically accompany blueshifted low-ionization lines (e.g., [147]). Star forming galaxies also show an increase in the velocity of Lyα as SFR and Lyα equivalent width increase [185–187]. However, whether this is due solely to changing outflow properties or instead to an increase in gas near the systemic redshift is unclear [187].

Finally, a handful of molecular gas detections of outflows at moderate-to-high z are emerging. CO has been imaged in two high-velocity, apparently stellar GWs in post-starbursts at $z \sim 0.7$ [32,188]. A long *Herschel* integration allowed detection of an OH outflow in absorption in a $z = 2.3$ ULIRG [189]. A serendipitous ALMA discovery of extremely broad CH^+ in several $z \sim 2.5$ ULIRGs points to turbulent outflows [190]. Tentative detections of broad, faint [C II] line wings at $z = 5.5$ hint at the possibility of stellar GWs in modestly star-forming galaxies at this epoch [191]. Finally, an OH outflow exists in a gravitationally lensed, dusty galaxy at $z = 5.3$ [192].

5. Summary

We can say with reasonable certainty that GWs driven by energy from stellar processes are a common feature of galaxies with moderate-to-high star formation rates and/or surface densities out to $z \sim 2 - 3$. Stacking analyses of large rest-frame UV and optical spectroscopic surveys have established that the average star-forming galaxy has an ionized and/or neutral wind whose velocity scales with star formation rate, stellar mass, and possibly $\Sigma_{\rm SFR}$. At low redshift, these winds are most prominent in starburst galaxies that lie above the galaxy main sequence; at higher redshift, where galaxies on the main sequence have higher SFR, the situation may be different. Hints exist that GWs are common but simply hard to detect even in galaxies with low $\Sigma_{\rm SFR}$ (for instance, the low-surface-brightness Milky Way GW).

The correlations between outflow and galaxy properties found in some of the first large surveys of stellar GWs have been verified and refined by larger and more diverse samples and different gas probes. Besides serving merely as input to parameterizations of outflows in numerical simulations, measurements of GWs can now be compared to the predicted properties of GWs from simulations that better implement the physics of stellar feedback.

Detailed, multiwavelength studies of star-forming galaxies continue to reveal new layers of GWs. Most notable is that stellar GWs entrain large quantities of molecular gas, including dense clumps, and loft dust and soot (PAHs) far above the galactic disk. The promising technique of combining resonant-line absorption and emission with non-resonant re-emission channels has been successfully used to detect winds at high z and may prove a powerful probe of GW structure and extent when widely deployed. Observations of a wider range of galaxies besides the usual suspects (e.g., M82) with 3D imaging spectroscopy shows that a complex, multiphase structure of filaments of dusty ionized and neutral gas collimated along the minor axis is a common feature of GWs. Transverse-sightline spectroscopy and correlations with galaxy inclination at a variety of redshifts bolster this picture. Finally, increasingly in-depth studies of local galaxies with extended Lyα and LyC may eventually put meaningful constraints on how outflows contribute to reionization and help interpret high-z observations of Lyα.

Future progress will occur on a variety of fronts. At low z, a new generation of ongoing multi-object IFS surveys (SAMI Galaxy Survey, MaNGA) will soon produce results on thousands of nearby galaxies. Future, much larger IFS surveys are being planned (using, e.g., Hector; [193]). Sensitive, wide-field IFS instruments on large telescopes (such as MUSE and KCWI, the Keck Cosmic Web Imager) will probe the full extent of GWs in nearby, well-resolved targets and enable efficient, spatially resolved characterization of many galaxies at once in high-z deep fields. Next generation multi-object spectroscopy surveys (e.g., the Dark Energy Spectroscopic Instrument, or DESI, Survey and 4MOST, the 4-metre Multi-Object Spectroscopic Telescope) will increase the fidelity of stacking analyses over a wider range of redshift and galaxy properties.

Continued measurements with ALMA, particularly at high spatial resolution, will provide more detailed understanding of the structure and chemistry of molecular gas in outflows. ALMA will also certainly expand on its currently short list of detections of high-z stellar GWs. The high resolution and sensitivity of the *James Webb Space Telescope* (*JWST*) in the MIR will undoubtedly produce useful measurements of molecular gas and dust in stellar GWs, as well. However, the spatial resolution and sensitivity of *JWST* is likely to provide the most dramatic advances in measuring the properties of outflows in high-z galaxies by characterizing them in individual main-sequence galaxies at $z \sim 2-3$ and detecting them at very high z, where their impact could be especially significant but where measurements currently do not exist.

Finally, we note two areas of study that have seen little recent progress, but whose prospects should eventually rise. Measurements of the radio-emitting plasma in GWs are very rare except for a few recent detections [194–196]. The next generation of wide-field radio arrays may make this a growth area. The field of X-rays studies of GWs has also lain fallow, with a few exceptions (e.g., [197,198]). The hottest gas phase of GWs, which may drive the outflows in starburst galaxies, has proven extremely difficult to detect except in the nearest cases [27]. More sensitive X-ray telescopes in the coming two decades will eventually lead to a better characterization of this pivotal component.

Acknowledgments: The author thanks the referees for their feedback.

Funding: This research received no external funding. The author is supported by the J. Lester Crain chair at Rhodes College.

Conflicts of Interest: The author declares no conflict of interest.

Abbreviations

The following abbreviations are used in this manuscript:

ALMA	Atacama Large Millimeter/submillimeter Array
COS	Cosmic Origins Spectrograph
FIR	far-infrared
GW	galactic wind
IFS	integral field spectrograph
LBG	Lyman-break galaxy
LIRG	luminous infrared galaxy
MIR	mid-infrared
NIR	near-infrared
SFR	star formation rate
sSFR	specific star formation rate
ULIRG	ultraluminous infrared galaxy

References

1. Heckman, T.M.; Lehnert, M.D.; Armus, L. Galactic Superwinds. In *The Environment and Evolution of Galaxies*; Shull, J.M., Thronson, H.A., Eds.; Springer Netherlands: Dordrecht, Netherlands, 1993; Volume 188, p. 455.
2. Veilleux, S.; Cecil, G.; Bland-Hawthorn, J. Galactic Winds. *Annu. Revs. Astron. Astrophys.* **2005**, *43*, 769–826.
3. Zahid, H.J.; Torrey, P.; Vogelsberger, M.; Hernquist, L.; Kewley, L.; Davé, R. Empirical constraints for the magnitude and composition of galactic winds. *Astrophys. Space Sci.* **2014**, *349*, 873–879.
4. Tumlinson, J.; Thom, C.; Werk, J.K.; Prochaska, J.X.; Tripp, T.M.; Weinberg, D.H.; Peeples, M.S.; O'Meara, J.M.; Oppenheimer, B.D.; Meiring, J.D.; et al. The Large, Oxygen-Rich Halos of Star-Forming Galaxies Are a Major Reservoir of Galactic Metals. *Science* **2011**, *334*, 948–952.
5. Borthakur, S.; Heckman, T.; Strickland, D.; Wild, V.; Schiminovich, D. The Impact of Starbursts on the Circumgalactic Medium. *Astrophys. J.* **2013**, *768*, 18.
6. Bordoloi, R.; Tumlinson, J.; Werk, J.K.; Oppenheimer, B.D.; Peeples, M.S.; Prochaska, J.X.; Tripp, T.M.; Katz, N.; Davé, R.; Fox, A.J.; et al. The COS-Dwarfs Survey: The Carbon Reservoir around Sub-L* Galaxies. *Astrophys. J.* **2014**, *796*, 136.
7. Borthakur, S.; Heckman, T.; Tumlinson, J.; Bordoloi, R.; Kauffmann, G.; Catinella, B.; Schiminovich, D.; Davé, R.; Moran, S.M.; Saintonge, A. The Properties of the Circumgalactic Medium in Red and Blue Galaxies: Results from the COS-GASS+COS-Halos Surveys. *Astrophys. J.* **2016**, *833*, 259.
8. Heckman, T.; Borthakur, S.; Wild, V.; Schiminovich, D.; Bordoloi, R. COS-burst: Observations of the Impact of Starburst-driven Winds on the Properties of the Circum-galactic Medium. *Astrophys. J.* **2017**, *846*, 151.
9. Li, J.T.; Wang, Q.D. Chandra survey of nearby highly inclined disc galaxies—II. Correlation analysis of galactic coronal properties. *Mon. Not. R. Astron. Soc.* **2013**, *435*, 3071–3084.
10. Oppenheimer, B.D.; Davé, R.; Kereš, D.; Fardal, M.; Katz, N.; Kollmeier, J.A.; Weinberg, D.H. Feedback and recycled wind accretion: Assembling the z = 0 galaxy mass function. *Mon. Not. R. Astron. Soc.* **2010**, *406*, 2325–2338.
11. Hopkins, P.F.; Kereš, D.; Oñorbe, J.; Faucher-Giguère, C.A.; Quataert, E.; Murray, N.; Bullock, J.S. Galaxies on FIRE (Feedback In Realistic Environments): Stellar feedback explains cosmologically inefficient star formation. *Mon. Not. R. Astron. Soc.* **2014**, *445*, 581–603.
12. Anglés-Alcázar, D.; Davé, R.; Özel, F.; Oppenheimer, B.D. Cosmological Zoom Simulations of z = 2 Galaxies: The Impact of Galactic Outflows. *Astrophys. J.* **2014**, *782*, 84.
13. Fabian, A.C. Observational Evidence of Active Galactic Nuclei Feedback. *Annu. Revs. Astron. Astrophys.* **2012**, *50*, 455–489.
14. Harrison, C.M. Impact of supermassive black hole growth on star formation. *Nat. Astron.* **2017**, *1*, 0165.
15. Aird, J.; Coil, A.L.; Moustakas, J.; Blanton, M.R.; Burles, S.M.; Cool, R.J.; Eisenstein, D.J.; Smith, M.S.M.; Wong, K.C.; Zhu, G. PRIMUS: The Dependence of AGN Accretion on Host Stellar Mass and Color. *Astrophys. J.* **2012**, *746*, 90.
16. Jones, M.L.; Hickox, R.C.; Black, C.S.; Hainline, K.N.; DiPompeo, M.A.; Goulding, A.D. The Intrinsic Eddington Ratio Distribution of Active Galactic Nuclei in Star-forming Galaxies from the Sloan Digital Sky Survey. *Astrophys. J.* **2016**, *826*, 12.

17. Madau, P.; Dickinson, M. Cosmic Star-Formation History. *Annu. Revs. Astron. Astrophys.* **2014**, *52*, 415–486.
18. Tacconi, L.J.; Neri, R.; Genzel, R.; Combes, F.; Bolatto, A.; Cooper, M.C.; Wuyts, S.; Bournaud, F.; Burkert, A.; Comerford, J.; et al. Phibss: Molecular Gas Content and Scaling Relations in z ~1-3 Massive, Main-sequence Star-forming Galaxies. *Astrophys. J.* **2013**, *768*, 74.
19. van Dokkum, P.G.; Nelson, E.J.; Franx, M.; Oesch, P.; Momcheva, I.; Brammer, G.; Förster Schreiber, N.M.; Skelton, R.E.; Whitaker, K.E.; van der Wel, A.; et al. Forming Compact Massive Galaxies. *Astrophys. J.* **2015**, *813*, 23.
20. Nelson, E.J.; van Dokkum, P.G.; Förster Schreiber, N.M.; Franx, M.; Brammer, G.B.; Momcheva, I.G.; Wuyts, S.; Whitaker, K.E.; Skelton, R.E.; Fumagalli, M.; et al. Where Stars Form: Inside-out Growth and Coherent Star Formation from HST Hα Maps of 3200 Galaxies across the Main Sequence at $0.7 < z < 1.5$. *Astrophys. J.* **2016**, *828*, 27.
21. Lehnert, M.D.; Heckman, T.M. Ionized Gas in the Halos of Edge-on Starburst Galaxies: Evidence for Supernova-driven Superwinds. *Astrophys. J.* **1996**, *462*, 651.
22. Martin, C.L. The Impact of Star Formation on the Interstellar Medium in Dwarf Galaxies. II. The Formation of Galactic Winds. *Astrophys. J.* **1998**, *506*, 222–252.
23. Rupke, D.S.; Veilleux, S.; Sanders, D.B. Outflows in Infrared-Luminous Starbursts at $z < 0.5$. II. Analysis and Discussion. *Astrophys. J. Suppl. Ser.* **2005**, *160*, 115–148.
24. Veilleux, S.; Cecil, G.; Bland-Hawthorn, J.; Tully, R.B.; Filippenko, A.V.; Sargent, W.L.W. The Nuclear Superbubble of NGC 3079. *Astrophys. J.* **1994**, *433*, 48.
25. Lehnert, M.D.; Heckman, T.M.; Weaver, K.A. Very Extended X-Ray and Hα Emission in M82: Implications for the Superwind Phenomenon. *Astrophys. J.* **1999**, *523*, 575–584.
26. Veilleux, S.; Rupke, D.S. Identification of Galactic Wind Candidates Using Excitation Maps: Tunable-Filter Discovery of a Shock-excited Wind in the Galaxy NGC 1482. *Astrophys. J.* **2002**, *565*, L63–L66.
27. Strickland, D.K.; Heckman, T.M. Supernova Feedback Efficiency and Mass Loading in the Starburst and Galactic Superwind Exemplar M82. *Astrophys. J.* **2009**, *697*, 2030–2056.
28. Chisholm, J.; Tremonti, C.A.; Leitherer, C.; Chen, Y.; Wofford, A.; Lundgren, B. Scaling Relations between Warm Galactic Outflows and Their Host Galaxies. *Astrophys. J.* **2015**, *811*, 149.
29. Heckman, T.M.; Borthakur, S. The Implications of Extreme Outflows from Extreme Starbursts. *Astrophys. J.* **2016**, *822*, 9.
30. Heckman, T.M.; Alexandroff, R.M.; Borthakur, S.; Overzier, R.; Leitherer, C. The Systematic Properties of the Warm Phase of Starburst-Driven Galactic Winds. *Astrophys. J.* **2015**, *809*, 147.
31. Sell, P.H.; Tremonti, C.A.; Hickox, R.C.; Diamond- Stanic, A.M.; Moustakas, J.; Coil, A.; Williams, A.; Rudnick, G.; Robaina, A.; Geach, J.E.; et al. Massive compact galaxies with high-velocity outflows: Morphological analysis and constraints on AGN activity. *Mon. Not. R. Astron. Soc.* **2014**, *441*, 3417–3443.
32. Geach, J.E.; Hickox, R.C.; Diamond-Stanic, A.M.; Krips, M.; Rudnick, G.H.; Tremonti, C.A.; Sell, P.H.; Coil, A.L.; Moustakas, J. Stellar feedback as the origin of an extended molecular outflow in a starburst galaxy. *Nature* **2014**, *516*, 68–70.
33. Martin, C.L. Mapping Large-Scale Gaseous Outflows in Ultraluminous Galaxies with Keck II ESI Spectra: Variations in Outflow Velocity with Galactic Mass. *Astrophys. J.* **2005**, *621*, 227–245.
34. Cazzoli, S.; Arribas, S.; Maiolino, R.; Colina, L. Neutral gas outflows in nearby [U]LIRGs via optical NaD feature. *Astron. Astrophys.* **2016**, *590*, A125.
35. Arribas, S.; Colina, L.; Bellocchi, E.; Maiolino, R.; Villar-Martín, M. Ionized gas outflows and global kinematics of low-z luminous star- forming galaxies. *Astron. Astrophys.* **2014**, *568*, A14.
36. Chisholm, J.; Tremonti, C.A.; Leitherer, C.; Chen, Y. The mass and momentum outflow rates of photoionized galactic outflows. *Mon. Not. R. Astron. Soc.* **2017**, *469*, 4831–4849.
37. Reyes, R.; Mandelbaum, R.; Gunn, J.E.; Pizagno, J.; Lackner, C.N. Calibrated Tully-Fisher relations for improved estimates of disc rotation velocities. *Mon. Not. R. Astron. Soc.* **2011**, *417*, 2347–2386.
38. Hopkins, P.F.; Quataert, E.; Murray, N. Stellar feedback in galaxies and the origin of galaxy-scale winds. *Mon. Not. R. Astron. Soc.* **2012**, *421*, 3522–3537.
39. Lagos, C.D.P.; Lacey, C.G.; Baugh, C.M. A dynamical model of supernova feedback: Gas outflows from the interstellar medium. *Mon. Not. R. Astron. Soc.* **2013**, *436*, 1787–1817.
40. Tanner, R.; Cecil, G.; Heitsch, F. Scaling Relations of Starburst-Driven Galactic Winds. *Astrophys. J.* **2017**, *843*, 137.

41. Muratov, A.L.; Kereš, D.; Faucher- Giguère, C.A.; Hopkins, P.F.; Quataert, E.; Murray, N. Gusty, gaseous flows of FIRE: Galactic winds in cosmological simulations with explicit stellar feedback. *Mon. Not. R. Astron. Soc.* **2015**, *454*, 2691–2713.
42. Mitra, S.; Davé, R.; Finlator, K. Equilibrium model constraints on baryon cycling across cosmic time. *Mon. Not. R. Astron. Soc.* **2015**, *452*, 1184–1200.
43. Wofford, A.; Leitherer, C.; Salzer, J. Lyα Escape from z ~0.03 Star-forming Galaxies: The Dominant Role of Outflows. *Astrophys. J.* **2013**, *765*, 118.
44. Martin, C.L.; Dijkstra, M.; Henry, A.; Soto, K.T.; Danforth, C.W.; Wong, J. The Lyα Line Profiles of Ultraluminous Infrared Galaxies: Fast Winds and Lyman Continuum Leakage. *Astrophys. J.* **2015**, *803*, 6.
45. Rivera-Thorsen, T.E.; Hayes, M.; Östlin, G.; Duval, F.; Orlitová, I.; Verhamme, A.; Mas-Hesse, J.M.; Schaerer, D.; Cannon, J.M.; Otí-Floranes, H.; et al. The Lyman Alpha Reference Sample. V. The Impact of Neutral ISM Kinematics and Geometry on Lyα Escape. *Astrophys. J.* **2015**, *805*, 14.
46. Henry, A.; Scarlata, C.; Martin, C.L.; Erb, D. Lyα Emission from Green Peas: The Role of Circumgalactic Gas Density, Covering, and Kinematics. *Astrophys. J.* **2015**, *809*, 19.
47. Alexandroff, R.M.; Heckman, T.M.; Borthakur, S.; Overzier, R.; Leitherer, C. Indirect Evidence for Escaping Ionizing Photons in Local Lyman Break Galaxy Analogs. *Astrophys. J.* **2015**, *810*, 104.
48. Chisholm, J.; Orlitová, I.; Schaerer, D.; Verhamme, A.; Worseck, G.; Izotov, Y.I.; Thuan, T.X.; Guseva, N.G. Do galaxies that leak ionizing photons have extreme outflows? *Astron. Astrophys.* **2017**, *605*, A67.
49. Jaskot, A.E.; Oey, M.S.; Scarlata, C.; Dowd, T. Kinematics and Optical Depth in the Green Peas: Suppressed Superwinds in Candidate LyC Emitters. *Astrophys. J.* **2017**, *851*, L9.
50. Chen, Y.M.; Tremonti, C.A.; Heckman, T.M.; Kauffmann, G.; Weiner, B.J.; Brinchmann, J.; Wang, J. Absorption-line Probes of the Prevalence and Properties of Outflows in Present-day Star-forming Galaxies. *Astron. J.* **2010**, *140*, 445–461.
51. Cicone, C.; Maiolino, R.; Marconi, A. Outflows and complex stellar kinematics in SDSS star-forming galaxies. *Astron. Astrophys.* **2016**, *588*, A41.
52. Kauffmann, G.; Heckman, T.M.; Tremonti, C.; Brinchmann, J.; Charlot, S.; White, S.D.M.; Ridgway, S.E.; Brinkmann, J.; Fukugita, M.; Hall, P.B.; et al. The host galaxies of active galactic nuclei. *Mon. Not. R. Astron. Soc.* **2003**, *346*, 1055–1077.
53. Concas, A.; Popesso, P.; Brusa, M.; Mainieri, V.; Erfanianfar, G.; Morselli, L. Light breeze in the local Universe. *Astron. Astrophys.* **2017**, *606*, A36.
54. Stasińska, G.; Cid Fernandes, R.; Mateus, A.; Sodré, L.; Asari, N.V. Semi-empirical analysis of Sloan Digital Sky Survey galaxies—III. How to distinguish AGN hosts. *Mon. Not. R. Astron. Soc.* **2006**, *371*, 972–982.
55. Rich, J.A.; Dopita, M.A.; Kewley, L.J.; Rupke, D.S.N. NGC 839: Shocks in an M82-like Superwind. *Astrophys. J.* **2010**, *721*, 505–517.
56. Fogarty, L.M.R.; Bland-Hawthorn, J.; Croom, S.M.; Green, A.W.; Bryant, J.J.; Lawrence, J.S.; Richards, S.; Allen, J.T.; Bauer, A.E.; Birchall, M.N.; et al. First Science with SAMI: A Serendipitously Discovered Galactic Wind in ESO 185-G031. *Astrophys. J.* **2012**, *761*, 169.
57. Rupke, D.S.N.; Veilleux, S. The Multiphase Structure and Power Sources of Galactic Winds in Major Mergers. *Astrophys. J.* **2013**, *768*, 75.
58. Vogt, F.P.A.; Dopita, M.A.; Kewley, L.J. Galaxy Interactions in Compact Groups. I. The Galactic Winds of HCG16. *Astrophys. J.* **2013**, *768*, 151.
59. Ho, I.T.; Kewley, L.J.; Dopita, M.A.; Medling, A.M.; Allen, J.T.; Bland-Hawthorn, J.; Bloom, J.V.; Bryant, J.J.; Croom, S.M.; Fogarty, L.M.R.; et al. The SAMI Galaxy Survey: Shocks and outflows in a normal star-forming galaxy. *Mon. Not. R. Astron. Soc.* **2014**, *444*, 3894–3910.
60. Medling, A.M.; U, V.; Rich, J.A.; Kewley, L.J.; Armus, L.; Dopita, M.A.; Max, C.E.; Sanders, D.; Sutherland, R. Shocked gas in IRAS F17207-0014: ISM collisions and outflows. *Mon. Not. R. Astron. Soc.* **2015**, *448*, 2301–2311.
61. Martín-Fernández, P.; Jiménez-Vicente, J.; Zurita, A.; Mediavilla, E.; Castillo- Morales, Á. The multiphase starburst-driven galactic wind in NGC 5394. *Mon. Not. R. Astron. Soc.* **2016**, *461*, 6–21.
62. López-Cobá, C.; Sánchez, S.F.; Moiseev, A.V.; Oparin, D.V.; Bitsakis, T.; Cruz-González, I.; Morisset, C.; Galbany, L.; Bland-Hawthorn, J.; Roth, M.M.; et al. Star formation driven galactic winds in UGC 10043. *Mon. Not. R. Astron. Soc.* **2017**, *467*, 4951–4964.

63. Cresci, G.; Vanzi, L.; Telles, E.; Lanzuisi, G.; Brusa, M.; Mingozzi, M.; Sauvage, M.; Johnson, K. The MUSE view of He 2-10: No AGN ionization but a sparkling starburst. *Astron. Astrophys.* **2017**, *604*, A101.
64. Cortijo-Ferrero, C.; González Delgado, R.M.; Pérez, E.; Sánchez, S.F.; Cid Fernandes, R.; de Amorim, A.L.; Di Matteo, P.; García-Benito, R.; Lacerda, E.A.D.; López Fernández, R.; et al. The spatially resolved stellar population and ionized gas properties in the merger LIRG NGC 2623. *Astron. Astrophys.* **2017**, *606*, A95.
65. Rich, J.A.; Kewley, L.J.; Dopita, M.A. Composite Spectra in Merging U/LIRGs Caused by Shocks. *Astrophys. J.* **2014**, *781*, L12.
66. Rich, J.A.; Kewley, L.J.; Dopita, M.A. Galaxy Mergers Drive Shocks: An Integral Field Study of GOALS Galaxies. *Astrophys. J. Suppl. Ser.* **2015**, *221*, 28.
67. Soto, K.T.; Martin, C.L.; Prescott, M.K.M.; Armus, L. The Emission-line Spectra of Major Mergers: Evidence for Shocked Outflows. *Astrophys. J.* **2012**, *757*, 86.
68. Bryant, J.J.; Owers, M.S.; Robotham, A.S.G.; Croom, S.M.; Driver, S.P.; Drinkwater, M.J.; Lorente, N.P.F.; Cortese, L.; Scott, N.; Colless, M.; et al. The SAMI Galaxy Survey: Instrument specification and target selection. *Mon. Not. R. Astron. Soc.* **2015**, *447*, 2857–2879.
69. Bundy, K.; Bershady, M.A.; Law, D.R.; Yan, R.; Drory, N.; MacDonald, N.; Wake, D.A.; Cherinka, B.; Sánchez-Gallego, J.R.; Weijmans, A.M.; et al. Overview of the SDSS-IV MaNGA Survey: Mapping nearby Galaxies at Apache Point Observatory. *Astrophys. J.* **2015**, *798*, 7.
70. Ho, I.T.; Medling, A.M.; Bland-Hawthorn, J.; Groves, B.; Kewley, L.J.; Kobayashi, C.; Dopita, M.A.; Leslie, S.K.; Sharp, R.; Allen, J.T.; et al. The SAMI Galaxy Survey: Extraplanar gas, galactic winds and their association with star formation history. *Mon. Not. R. Astron. Soc.* **2016**, *457*, 1257–1278.
71. Tescari, E.; Cortese, L.; Power, C.; Wyithe, J.S.B.; Ho, I.T.; Crain, R.A.; Bland-Hawthorn, J.; Croom, S.M.; Kewley, L.J.; Schaye, J.; et al. The SAMI Galaxy Survey: Understanding observations of large-scale outflows at low redshift with EAGLE simulations. *Mon. Not. R. Astron. Soc.* **2018**, *473*, 380–397.
72. Tsai, A.L.; Matsushita, S.; Nakanishi, K.; Kohno, K.; Kawabe, R.; Inui, T.; Matsumoto, H.; Tsuru, T.G.; Peck, A.B.; Tarchi, A. Molecular Superbubbles and Outflows from the Starburst Galaxy NGC 2146. *Publ. Astron. Soc. Jpn.* **2009**, *61*, 237.
73. Sakamoto, K.; Aalto, S.; Combes, F.; Evans, A.; Peck, A. An Infrared-luminous Merger with Two Bipolar Molecular Outflows: ALMA and SMA Observations of NGC 3256. *Astrophys. J.* **2014**, *797*, 90.
74. Cicone, C.; Maiolino, R.; Sturm, E.; Graciá-Carpio, J.; Feruglio, C.; Neri, R.; Aalto, S.; Davies, R.; Fiore, F.; Fischer, J.; et al. Massive molecular outflows and evidence for AGN feedback from CO observations. *Astron. Astrophys.* **2014**, *562*, A21.
75. García-Burillo, S.; Combes, F.; Usero, A.; Aalto, S.; Colina, L.; Alonso-Herrero, A.; Hunt, L.K.; Arribas, S.; Costagliola, F.; Labiano, A.; et al. High-resolution imaging of the molecular outflows in two mergers: IRAS 17208-0014 and NGC 1614. *Astron. Astrophys.* **2015**, *580*, A35.
76. Pereira-Santaella, M.; Colina, L.; García-Burillo, S.; Alonso-Herrero, A.; Arribas, S.; Cazzoli, S.; Emonts, B.; Piqueras López, J.; Planesas, P.; Storchi Bergmann, T.; et al. High-velocity extended molecular outflow in the star-formation dominated luminous infrared galaxy ESO 320-G030. *Astron. Astrophys.* **2016**, *594*, A81.
77. Sakamoto, K.; Aalto, S.; Barcos-Muñoz, L.; Costagliola, F.; Evans, A.S.; Harada, N.; Martín, S.; Wiedner, M.; Wilner, D. Resolved Structure of the Arp 220 Nuclei at $\lambda \approx 3$ mm. *Astrophys. J.* **2017**, *849*, 14.
78. Barcos-Muñoz, L.; Aalto, S.; Thompson, T.A.; Sakamoto, K.; Martín, S.; Leroy, A.K.; Privon, G.C.; Evans, A.S.; Kepley, A. Fast, Collimated Outflow in the Western Nucleus of Arp 220. *Astrophys. J.* **2018**, *853*, L28.
79. Falstad, N.; Aalto, S.; Mangum, J.G.; Costagliola, F.; Gallagher, J.S.; González-Alfonso, E.; Sakamoto, K.; König, S.; Muller, S.; Evans, A.S.; et al. Hidden molecular outflow in the LIRG Zw 049.057. *Astron. Astrophys.* **2018**, *609*, A75.
80. Tsai, A.L.; Matsushita, S.; Kong, A.K.H.; Matsumoto, H.; Kohno, K. First Detection of a Subkiloparsec Scale Molecular Outflow in the Starburst Galaxy NGC 3628. *Astrophys. J.* **2012**, *752*, 38.
81. Bolatto, A.D.; Warren, S.R.; Leroy, A.K.; Walter, F.; Veilleux, S.; Ostriker, E.C.; Ott, J.; Zwaan, M.; Fisher, D.B.; Weiss, A.; et al. Suppression of star formation in the galaxy NGC 253 by a starburst- driven molecular wind. *Nature* **2013**, *499*, 450–453.
82. Leroy, A.K.; Walter, F.; Martini, P.; Roussel, H.; Sandstrom, K.; Ott, J.; Weiss, A.; Bolatto, A.D.; Schuster, K.; Dessauges-Zavadsky, M. The Multi-phase Cold Fountain in M82 Revealed by a Wide, Sensitive Map of the Molecular Interstellar Medium. *Astrophys. J.* **2015**, *814*, 83.

83. Salak, D.; Nakai, N.; Hatakeyama, T.; Miyamoto, Y. Gas Dynamics and Outflow in the Barred Starburst Galaxy NGC 1808 Revealed with ALMA. *Astrophys. J.* **2016**, *823*, 68.
84. García-Burillo, S.; Martín-Pintado, J.; Fuente, A.; Neri, R. SiO Chimneys and Supershells in M82. *Astrophys. J.* **2001**, *563*, L27–L30.
85. Walter, F.; Weiss, A.; Scoville, N. Molecular Gas in M82: Resolving the Outflow and Streamers. *Astrophys. J.* **2002**, *580*, L21–L25.
86. Strickland, D.K.; Heckman, T.M.; Weaver, K.A.; Dahlem, M. Chandra Observations of NGC 253: New Insights into the Nature of Starburst-driven Superwinds. *Astron. J.* **2000**, *120*, 2965–2974.
87. Salas, P.; Galaz, G.; Salter, D.; Herrera-Camus, R.; Bolatto, A.D.; Kepley, A. Extended HCN and HCO^+ Emission in the Starburst Galaxy M82. *Astrophys. J.* **2014**, *797*, 134.
88. Kepley, A.A.; Leroy, A.K.; Frayer, D.; Usero, A.; Marvil, J.; Walter, F. The Green Bank Telescope Maps the Dense, Star-forming Gas in the Nearby Starburst Galaxy M82. *Astrophys. J.* **2014**, *780*, L13.
89. Walter, F.; Bolatto, A.D.; Leroy, A.K.; Veilleux, S.; Warren, S.R.; Hodge, J.; Levy, R.C.; Meier, D.S.; Ostriker, E.C.; Ott, J.; et al. Dense Molecular Gas Tracers in the Outflow of the Starburst Galaxy NGC 253. *Astrophys. J.* **2017**, *835*, 265.
90. Salak, D.; Tomiyasu, Y.; Nakai, N.; Kuno, N.; Miyamoto, Y.; Kaneko, H. Dense Molecular Gas in the Starburst Nucleus of NGC 1808. *Astrophys. J.* **2018**, *856*, 97.
91. Sakamoto, K.; Aalto, S.; Wilner, D.J.; Black, J.H.; Conway, J.E.; Costagliola, F.; Peck, A.B.; Spaans, M.; Wang, J.; Wiedner, M.C. P Cygni Profiles of Molecular Lines Toward Arp 220 Nuclei. *Astrophys. J.* **2009**, *700*, L104–L108.
92. Tunnard, R.; Greve, T.R.; Garcia-Burillo, S.; Graciá Carpio, J.; Fischer, J.; Fuente, A.; González-Alfonso, E.; Hailey-Dunsheath, S.; Neri, R.; Sturm, E.; et al. Chemically Distinct Nuclei and Outflowing Shocked Molecular Gas in Arp 220. *Astrophys. J.* **2015**, *800*, 25.
93. Zschaechner, L.K.; Ott, J.; Walter, F.; Meier, D.S.; Momjian, E.; Scoville, N. High-resolution Observations of Molecular Lines in Arp 220: Kinematics, Morphology, and Limits on the Applicability of the Ammonia Thermometer. *Astrophys. J.* **2016**, *833*, 41.
94. Martín, S.; Aalto, S.; Sakamoto, K.; González- Alfonso, E.; Muller, S.; Henkel, C.; García-Burillo, S.; Aladro, R.; Costagliola, F.; Harada, N.; et al. The unbearable opaqueness of Arp220. *Astron. Astrophys.* **2016**, *590*, A25.
95. Rangwala, N.; Maloney, P.R.; Glenn, J.; Wilson, C.D.; Rykala, A.; Isaak, K.; Baes, M.; Bendo, G.J.; Boselli, A.; Bradford, C.M.; et al. Observations of Arp 220 Using Herschel-SPIRE: An Unprecedented View of the Molecular Gas in an Extreme Star Formation Environment. *Astrophys. J.* **2011**, *743*, 94.
96. Sturm, E.; González-Alfonso, E.; Veilleux, S.; Fischer, J.; Graciá-Carpio, J.; Hailey- Dunsheath, S.; Contursi, A.; Poglitsch, A.; Sternberg, A.; Davies, R.; et al. Massive Molecular Outflows and Negative Feedback in ULIRGs Observed by Herschel-PACS. *Astrophys. J.* **2011**, *733*, L16.
97. Spoon, H.W.W.; Farrah, D.; Lebouteiller, V.; Gonzá lez-Alfonso, E.; Bernard-Salas, J.; Urrutia, T.; Rigopoulou, D.; Westmoquette, M.S.; Smith, H.A.; Afonso, J.; et al. Diagnostics of AGN-Driven Molecular Outflows in ULIRGs from Herschel- PACS Observations of OH at 119 μm. *Astrophys. J.* **2013**, *775*, 127.
98. Veilleux, S.; Meléndez, M.; Sturm, E.; Gracia-Carpio, J.; Fischer, J.; González-Alfonso, E.; Contursi, A.; Lutz, D.; Poglitsch, A.; Davies, R.; et al. Fast Molecular Outflows in Luminous Galaxy Mergers: Evidence for Quasar Feedback from Herschel. *Astrophys. J.* **2013**, *776*, 27.
99. González-Alfonso, E.; Fischer, J.; Spoon, H.W.W.; Stewart, K.P.; Ashby, M.L.N.; Veilleux, S.; Smith, H.A.; Sturm, E.; Farrah, D.; Falstad, N.; et al. Molecular Outflows in Local ULIRGs: Energetics from Multitransition OH Analysis. *Astrophys. J.* **2017**, *836*, 11.
100. Janssen, A.W.; Christopher, N.; Sturm, E.; Veilleux, S.; Contursi, A.; González-Alfonso, E.; Fischer, J.; Davies, R.; Verma, A.; Graciá-Carpio, J.; et al. Broad [C II] Line Wings as Tracer of Molecular and Multi-phase Outflows in Infrared Bright Galaxies. *Astrophys. J.* **2016**, *822*, 43.
101. Rupke, D.S.; Veilleux, S.; Sanders, D.B. Outflows in Active Galactic Nucleus/Starburst-Composite Ultraluminous Infrared Galaxies1. *Astrophys. J.* **2005**, *632*, 751–780.
102. Contursi, A.; Poglitsch, A.; Grácia Carpio, J.; Veilleux, S.; Sturm, E.; Fischer, J.; Verma, A.; Hailey-Dunsheath, S.; Lutz, D.; Davies, R.; et al. Spectroscopic FIR mapping of the disk and galactic wind of M 82 with Herschel-PACS. *Astron. Astrophys.* **2013**, *549*, A118.

103. Kreckel, K.; Armus, L.; Groves, B.; Lyubenova, M.; Díaz-Santos, T.; Schinnerer, E.; Appleton, P.; Croxall, K.V.; Dale, D.A.; Hunt, L.K.; et al. A Far-IR View of the Starburst-driven Superwind in NGC 2146. *Astrophys. J.* **2014**, *790*, 26.
104. Krips, M.; Martín, S.; Sakamoto, K.; Aalto, S.; Bisbas, T.G.; Bolatto, A.D.; Downes, D.; Eckart, A.; Feruglio, C.; García-Burillo, S.; et al. ACA [CI] observations of the starburst galaxy NGC 253. *Astron. Astrophys.* **2016**, *592*, L3.
105. Martini, P.; Leroy, A.K.; Mangum, J.G.; Bolatto, A.; Keating, K.M.; Sandstrom, K.; Walter, F. H I Kinematics along the Minor Axis of M82. *Astrophys. J.* **2018**, *856*, 61.
106. Veilleux, S.; Rupke, D.S.N.; Swaters, R. Warm Molecular Hydrogen in the Galactic Wind of M82. *Astrophys. J.* **2009**, *700*, L149–L153.
107. Beirão, P.; Armus, L.; Lehnert, M.D.; Guillard, P.; Heckman, T.; Draine, B.; Hollenbach, D.; Walter, F.; Sheth, K.; Smith, J.D.; et al. Spatially resolved Spitzer-IRS spectral maps of the superwind in M82. *Mon. Not. R. Astron. Soc.* **2015**, *451*, 2640–2655.
108. Emonts, B.H.C.; Piqueras-López, J.; Colina, L.; Arribas, S.; Villar-Martín, M.; Pereira-Santaella, M.; Garcia-Burillo, S.; Alonso-Herrero, A. Outflow of hot and cold molecular gas from the obscured secondary nucleus of NGC 3256: Closing in on feedback physics. *Astron. Astrophys.* **2014**, *572*, A40.
109. Emonts, B.H.C.; Colina, L.; Piqueras-López, J.; Garcia-Burillo, S.; Pereira-Santaella, M.; Arribas, S.; Labiano, A.; Alonso-Herrero, A. Outflows of hot molecular gas in ultra-luminous infrared galaxies mapped with VLT-SINFONI. *Astron. Astrophys.* **2017**, *607*, A116.
110. Hill, M.J.; Zakamska, N.L. Warm molecular hydrogen in outflows from ultraluminous infrared Galaxies. *Mon. Not. R. Astron. Soc.* **2014**, *439*, 2701–2716.
111. Phillips, A.C. Nuclear and large-Scale Outflows in NGC 1808. *Astron. J.* **1993**, *105*, 486.
112. Hoopes, C.G.; Heckman, T.M.; Strickland, D.K.; Seibert, M.; Madore, B.F.; Rich, R.M.; Bianchi, L.; Gil de Paz, A.; Burgarella, D.; Thilker, D.A.; et al. GALEX Observations of the Ultraviolet Halos of NGC 253 and M82. *Astrophys. J.* **2005**, *619*, L99–L102.
113. Yoshida, M.; Kawabata, K.S.; Ohyama, Y. Spectropolarimetry of the Superwind Filaments of the Starburst Galaxy M 82: Kinematics of Dust Outflow. *Publ. Astron. Soc. Jpn.* **2011**, *63*, 493.
114. Hutton, S.; Ferreras, I.; Wu, K.; Kuin, P.; Breeveld, A.; Yershov, V.; Cropper, M.; Page, M. A panchromatic analysis of starburst galaxy M82: Probing the dust properties. *Mon. Not. R. Astron. Soc.* **2014**, *440*, 150–160.
115. Hutton, S.; Ferreras, I.; Yershov, V. Variations of the dust properties of M82 with galactocentric distance. *Mon. Not. R. Astron. Soc.* **2015**, *452*, 1412–1420.
116. Kaneda, H.; Ishihara, D.; Suzuki, T.; Ikeda, N.; Onaka, T.; Yamagishi, M.; Ohyama, Y.; Wada, T.; Yasuda, A. Large-scale distributions of mid- and far-infrared emission from the center to the halo of M 82 revealed with AKARI. *Astron. Astrophys.* **2010**, *514*, A14.
117. Roussel, H.; Wilson, C.D.; Vigroux, L.; Isaak, K.G.; Sauvage, M.; Madden, S.C.; Auld, R.; Baes, M.; Barlow, M.J.; Bendo, G.J.; et al. SPIRE imaging of M 82: Cool dust in the wind and tidal streams. *Astron. Astrophys.* **2010**, *518*, L66.
118. Leeuw, L.L.; Robson, E.I. Submillimeter Continuum Properties of Cold Dust in the Inner Disk and Outflows of M 82. *Astron. J.* **2009**, *137*, 517–527.
119. Kaneda, H.; Yamagishi, M.; Suzuki, T.; Onaka, T. AKARI Detection of Far-Infrared Dust Emission in the Halo of NGC 253. *Astrophys. J.* **2009**, *698*, L125–L128.
120. Meléndez, M.; Veilleux, S.; Martin, C.; Engelbracht, C.; Bland-Hawthorn, J.; Cecil, G.; Heitsch, F.; McCormick, A.; Müller, T.; Rupke, D.; et al. Exploring the Dust Content of Galactic Winds with Herschel. I. NGC 4631. *Astrophys. J.* **2015**, *804*, 46.
121. McCormick, A.; Veilleux, S.; Meléndez, M.; Martin, C.L.; Bland-Hawthorn, J.; Cecil, G.; Heitsch, F.; Müller, T.; Rupke, D.S.N.; Engelbracht, C. Exploring the dust content of galactic winds with Herschel—II. Nearby dwarf galaxies. *Mon. Not. R. Astron. Soc.* **2018**, *477*, 699–726.
122. Suzuki, T.; Kaneda, H.; Onaka, T.; Yamagishi, M.; Ishihara, D.; Kokusho, T.; Tsuchikawa, T. Enhanced dust emissivity power-law index along the western H α filament of NGC 1569. *Mon. Not. R. Astron. Soc.* **2018**, *477*, 3065–3075.
123. Engelbracht, C.W.; Kundurthy, P.; Gordon, K.D.; Rieke, G.H.; Kennicutt, R.C.; Smith, J.D.T.; Regan, M.W.; Makovoz, D.; Sosey, M.; Draine, B.T.; et al. Extended Mid-Infrared Aromatic Feature Emission in M82. *Astrophys. J.* **2006**, *642*, L127–L132.

124. Yamagishi, M.; Kaneda, H.; Ishihara, D.; Kondo, T.; Onaka, T.; Suzuki, T.; Minh, Y.C. AKARI near-infrared spectroscopy of the aromatic and aliphatic hydrocarbon emission features in the galactic superwind of M 82. *Astron. Astrophys.* **2012**, *541*, A10.
125. Onaka, T.; Matsumoto, H.; Sakon, I.; Kaneda, H. Detection of unidentified infrared bands in a Hα filament in the dwarf galaxy NGC 1569 with AKARI. *Astron. Astrophys.* **2010**, *514*, A15.
126. McCormick, A.; Veilleux, S.; Rupke, D.S.N. Dusty Winds: Extraplanar Polycyclic Aromatic Hydrocarbon Features of Nearby Galaxies. *Astrophys. J.* **2013**, *774*, 126.
127. Shopbell, P.L.; Bland-Hawthorn, J. The Asymmetric Wind in M82. *Astrophys. J.* **1998**, *493*, 129–153.
128. Lockhart, K.E.; Kewley, L.J.; Lu, J.R.; Allen, M.G.; Rupke, D.; Calzetti, D.; Davies, R.I.; Dopita, M.A.; Engel, H.; Heckman, T.M.; et al. HST/WFC3 Observations of an Off-nuclear Superbubble in Arp 220. *Astrophys. J.* **2015**, *810*, 149.
129. Rupke, D.S.N.; Veilleux, S. Breaking the Obscuring Screen: A Resolved Molecular Outflow in a Buried QSO. *Astrophys. J.* **2013**, *775*, L15.
130. Marconi, A.; Oliva, E.; van der Werf, P.P.; Maiolino, R.; Schreier, E.J.; Macchetto, F.; Moorwood, A.F.M. The elusive active nucleus of NGC 4945. *Astron. Astrophys.* **2000**, *357*, 24–36.
131. Su, M.; Slatyer, T.R.; Finkbeiner, D.P. Giant Gamma-ray Bubbles from Fermi-LAT: Active Galactic Nucleus Activity or Bipolar Galactic Wind? *Astrophys. J.* **2010**, *724*, 1044–1082.
132. Ackermann, M.; Albert, A.; Atwood, W.B.; Baldini, L.; Ballet, J.; Barbiellini, G.; Bastieri, D.; Bellazzini, R.; Bissaldi, E.; Blandford, R.D.; et al. The Spectrum and Morphology of the Fermi Bubbles. *Astrophys. J.* **2014**, *793*, 64.
133. Crocker, R.M.; Bicknell, G.V.; Taylor, A.M.; Carretti, E. A Unified Model of the Fermi Bubbles, Microwave Haze, and Polarized Radio Lobes: Reverse Shocks in the Galactic Center's Giant Outflows. *Astrophys. J.* **2015**, *808*, 107.
134. Yang, H.Y.; Ruszkowski, M.; Zweibel, E. Unveiling the Origin of the Fermi Bubbles. *Galaxies* **2018**, *6*, 29.
135. Carretti, E.; Crocker, R.M.; Staveley-Smith, L.; Haverkorn, M.; Purcell, C.; Gaensler, B.M.; Bernardi, G.; Kesteven, M.J.; Poppi, S. Giant magnetized outflows from the centre of the Milky Way. *Nature* **2013**, *493*, 66–69.
136. Planck Collaboration; Ade, P.A.R.; Aghanim, N.; Arnaud, M.; Ashdown, M.; Atrio-Barandela, F.; Aumont, J.; Baccigalupi, C.; Balbi, A.; Banday, A.J.; et al. Planck intermediate results. IX. Detection of the Galactic haze with Planck. *Astron. Astrophys.* **2013**, *554*, A139.
137. McClure-Griffiths, N.M.; Green, J.A.; Hill, A.S.; Lockman, F.J.; Dickey, J.M.; Gaensler, B.M.; Green, A.J. Atomic Hydrogen in a Galactic Center Outflow. *Astrophys. J.* **2013**, *770*, L4.
138. Lockman, F.J.; McClure-Griffiths, N.M. Tracing the Milky Way Nuclear Wind with 21cm Atomic Hydrogen Emission. *Astrophys. J.* **2016**, *826*, 215.
139. Di Teodoro, E.M.; McClure-Griffiths, N.M.; Lockman, F.J.; Denbo, S.R.; Endsley, R.; Ford, H.A.; Harrington, K. Blowing in the Milky Way Wind: Neutral Hydrogen Clouds Tracing the Galactic Nuclear Outflow. *Astrophys. J.* **2018**, *855*, 33.
140. Fang, T.; Jiang, X. High Resolution X-Ray Spectroscopy of the Local Hot Gas along the 3C 273 Sightline. *Astrophys. J.* **2014**, *785*, L24.
141. Bordoloi, R.; Fox, A.J.; Lockman, F.J.; Wakker, B.P.; Jenkins, E.B.; Savage, B.D.; Hernandez, S.; Tumlinson, J.; Bland- Hawthorn, J.; Kim, T.S. Mapping the Nuclear Outflow of the Milky Way: Studying the Kinematics and Spatial Extent of the Northern Fermi Bubble. *Astrophys. J.* **2017**, *834*, 191.
142. Savage, B.D.; Kim, T.S.; Fox, A.J.; Massa, D.; Bordoloi, R.; Jenkins, E.B.; Lehner, N.; Bland-Hawthorn, J.; Lockman, F.J.; Hernandez, S.; et al. Probing the Outflowing Multiphase Gas $\sim$1 kpc below the Galactic Center. *Astrophys. J. Suppl. Ser.* **2017**, *232*, 25.
143. Karim, M.T.; Fox, A.J.; Jenkins, E.B.; Bordoloi, R.; Wakker, B.P.; Savage, B.D.; Lockman, F.J.; Crawford, S.M.; Jorgenson, R.A.; Bland-Hawthorn, J. Probing the Southern Fermi Bubble in Ultraviolet Absorption Using Distant AGNs. *Astrophys. J.* **2018**, *860*, 98.
144. Barger, K.A.; Lehner, N.; Howk, J.C. Down-the-barrel and Transverse Observations of the Large Magellanic Cloud: Evidence for a Symmetric Galactic Wind on the Near and Far Sides of the Galaxy. *Astrophys. J.* **2016**, *817*, 91.
145. Pettini, M.; Steidel, C.C.; Adelberger, K.L.; Dickinson, M.; Giavalisco, M. The Ultraviolet Spectrum of MS 1512-CB58: An Insight into Lyman-Break Galaxies. *Astrophys. J.* **2000**, *528*, 96–107.

146. Pettini, M.; Shapley, A.E.; Steidel, C.C.; Cuby, J.G.; Dickinson, M.; Moorwood, A.F.M.; Adelberger, K.L.; Giavalisco, M. The Rest-Frame Optical Spectra of Lyman Break Galaxies: Star Formation, Extinction, Abundances, and Kinematics. *Astrophys. J.* **2001**, *554*, 981–1000.
147. Steidel, C.C.; Erb, D.K.; Shapley, A.E.; Pettini, M.; Reddy, N.; Bogosavljević, M.; Rudie, G.C.; Rakic, O. The Structure and Kinematics of the Circumgalactic Medium from Far- ultraviolet Spectra of z ~= 2-3 Galaxies. *Astrophys. J.* **2010**, *717*, 289–322.
148. Genzel, R.; Newman, S.; Jones, T.; Förster Schreiber, N.M.; Shapiro, K.; Genel, S.; Lilly, S.J.; Renzini, A.; Tacconi, L.J.; Bouché, N.; et al. The Sins Survey of z ~2 Galaxy Kinematics: Properties of the Giant Star-forming Clumps. *Astrophys. J.* **2011**, *733*, 101.
149. Le Tiran, L.; Lehnert, M.D.; van Driel, W.; Nesvadba, N.P.H.; Di Matteo, P. The average optical spectra of intense starbursts at z ~2: Outflows and the pressurization of the ISM. *Astron. Astrophys.* **2011**, *534*, L4.
150. Newman, S.F.; Shapiro Griffin, K.; Genzel, R.; Davies, R.; Förster-Schreiber, N.M.; Tacconi, L.J.; Kurk, J.; Wuyts, S.; Genel, S.; Lilly, S.J.; et al. Shocked Superwinds from the z ~2 Clumpy Star-forming Galaxy, ZC406690. *Astrophys. J.* **2012**, *752*, 111.
151. Newman, S.F.; Genzel, R.; Förster-Schreiber, N.M.; Shapiro Griffin, K.; Mancini, C.; Lilly, S.J.; Renzini, A.; Bouché, N.; Burkert, A.; Buschkamp, P.; et al. The SINS/zC-SINF Survey of z ~2 Galaxy Kinematics: Outflow Properties. *Astrophys. J.* **2012**, *761*, 43.
152. Wisnioski, E.; Mendel, J.T.; Förster Schreiber, N.M.; Genzel, R.; Wilman, D.; Wuyts, S.; Belli, S.; Beifiori, A.; Bender, R.; Brammer, G.; et al. The KMOS^{3D} Survey: Rotating Compact Star-forming Galaxies and the Decomposition of Integrated Line Widths. *Astrophys. J.* **2018**, *855*, 97.
153. Finley, H.; Bouché, N.; Contini, T.; Epinat, B.; Bacon, R.; Brinchmann, J.; Cantalupo, S.; Erroz-Ferrer, S.; Marino, R.A.; Maseda, M.; et al. Galactic winds with MUSE: A direct detection of Fe II* emission from a z = 1.29 galaxy. *Astron. Astrophys.* **2017**, *605*, A118.
154. Weiner, B.J.; Coil, A.L.; Prochaska, J.X.; Newman, J.A.; Cooper, M.C.; Bundy, K.; Conselice, C.J.; Dutton, A.A.; Faber, S.M.; Koo, D.C.; et al. Ubiquitous Outflows in DEEP2 Spectra of Star-Forming Galaxies at z = 1.4. *Astrophys. J.* **2009**, *692*, 187–211.
155. Rubin, K.H.R.; Weiner, B.J.; Koo, D.C.; Martin, C.L.; Prochaska, J.X.; Coil, A.L.; Newman, J.A. The Persistence of Cool Galactic Winds in High Stellar Mass Galaxies between z ~1.4 and ~1. *Astrophys. J.* **2010**, *719*, 1503–1525.
156. Banerji, M.; Chapman, S.C.; Smail, I.; Alaghband- Zadeh, S.; Swinbank, A.M.; Dunlop, J.S.; Ivison, R.J.; Blain, A.W. Luminous starbursts in the redshift desert at z 1-2: Star formation rates, masses and evidence for outflows. *Mon. Not. R. Astron. Soc.* **2011**, *418*, 1071–1088.
157. Kornei, K.A.; Shapley, A.E.; Martin, C.L.; Coil, A.L.; Lotz, J.M.; Schiminovich, D.; Bundy, K.; Noeske, K.G. The Properties and Prevalence of Galactic Outflows at z ~1 in the Extended Groth Strip. *Astrophys. J.* **2012**, *758*, 135.
158. Erb, D.K.; Quider, A.M.; Henry, A.L.; Martin, C.L. Galactic Outflows in Absorption and Emission: Near-ultraviolet Spectroscopy of Galaxies at $1 < z < 2$. *Astrophys. J.* **2012**, *759*, 26.
159. Martin, C.L.; Shapley, A.E.; Coil, A.L.; Kornei, K.A.; Bundy, K.; Weiner, B.J.; Noeske, K.G.; Schiminovich, D. Demographics and Physical Properties of Gas Outflows/Inflows at $0.4 < z < 1.4$. *Astrophys. J.* **2012**, *760*, 127.
160. Bradshaw, E.J.; Almaini, O.; Hartley, W.G.; Smith, K.T.; Conselice, C.J.; Dunlop, J.S.; Simpson, C.; Chuter, R.W.; Cirasuolo, M.; Foucaud, S.; et al. High-velocity outflows from young star-forming galaxies in the UKIDSS Ultra-Deep Survey. *Mon. Not. R. Astron. Soc.* **2013**, *433*, 194–208.
161. Bordoloi, R.; Lilly, S.J.; Hardmeier, E.; Contini, T.; Kneib, J.P.; Le Fevre, O.; Mainieri, V.; Renzini, A.; Scodeggio, M.; Zamorani, G.; et al. The Dependence of Galactic Outflows on the Properties and Orientation of zCOSMOS Galaxies at z ~1. *Astrophys. J.* **2014**, *794*, 130.
162. Rubin, K.H.R.; Prochaska, J.X.; Koo, D.C.; Phillips, A.C.; Martin, C.L.; Winstrom, L.O. Evidence for Ubiquitous Collimated Galactic-scale Outflows along the Star-forming Sequence at z ~0.5. *Astrophys. J.* **2014**, *794*, 156.
163. Finley, H.; Bouché, N.; Contini, T.; Paalvast, M.; Boogaard, L.; Maseda, M.; Bacon, R.; Blaizot, J.; Brinchmann, J.; Epinat, B.; et al. The MUSE Hubble Ultra Deep Field Survey. VII. Fe II* emission in star- forming galaxies. *Astron. Astrophys.* **2017**, *608*, A7.
164. Prochaska, J.X.; Kasen, D.; Rubin, K. Simple Models of Metal-line Absorption and Emission from Cool Gas Outflows. *Astrophys. J.* **2011**, *734*, 24.

165. Williams, C.C.; Giavalisco, M.; Lee, B.; Tundo, E.; Mobasher, B.; Nayyeri, H.; Ferguson, H.C.; Koekemoer, A.; Trump, J.R.; Cassata, P.; et al. The Interstellar Medium and Feedback in the Progenitors of the Compact Passive Galaxies at z ~2. *Astrophys. J.* **2015**, *800*, 21.
166. Sugahara, Y.; Ouchi, M.; Lin, L.; Martin, C.L.; Ono, Y.; Harikane, Y.; Shibuya, T.; Yan, R. Evolution of Galactic Outflows at z∼0–2 Revealed with SDSS, DEEP2, and Keck Spectra. *Astrophys. J.* **2017**, *850*, 51.
167. Du, X.; Shapley, A.E.; Reddy, N.A.; Jones, T.; Stark, D.P.; Steidel, C.C.; Strom, A.L.; Rudie, G.C.; Erb, D.K.; Ellis, R.S.; et al. The Redshift Evolution of Rest-UV Spectroscopic Properties in Lyman- break Galaxies at z 2-4. *Astrophys. J.* **2018**, *860*, 75.
168. Du, X.; Shapley, A.E.; Martin, C.L.; Coil, A.L. The Kinematics of C IV in Star-forming Galaxies at z $\approx$ 1.2. *Astrophys. J.* **2016**, *829*, 64.
169. Chisholm, J.; Bordoloi, R.; Rigby, J.R.; Bayliss, M. Feeding the fire: Tracing the mass-loading of 10^7 K galactic outflows with O VI absorption. *Mon. Not. R. Astron. Soc.* **2018**, *474*, 1688–1704.
170. Rubin, K.H.R.; Prochaska, J.X.; Ménard, B.; Murray, N.; Kasen, D.; Koo, D.C.; Phillips, A.C. Low-ionization Line Emission from a Starburst Galaxy: A New Probe of a Galactic-scale Outflow. *Astrophys. J.* **2011**, *728*, 55.
171. Kornei, K.A.; Shapley, A.E.; Martin, C.L.; Coil, A.L.; Lotz, J.M.; Weiner, B.J. Fine-structure Fe II* Emission and Resonant Mg II Emission in z ~1 Star-forming Galaxies. *Astrophys. J.* **2013**, *774*, 50.
172. Bordoloi, R.; Rigby, J.R.; Tumlinson, J.; Bayliss, M.B.; Sharon, K.; Gladders, M.G.; Wuyts, E. Spatially resolved galactic wind in lensed galaxy RCSGA 032727-132609. *Mon. Not. R. Astron. Soc.* **2016**, *458*, 1891–1908.
173. Coil, A.L.; Weiner, B.J.; Holz, D.E.; Cooper, M.C.; Yan, R.; Aird, J. Outflowing Galactic Winds in Post-starburst and Active Galactic Nucleus Host Galaxies at $0.2 < z < 0.8$. *Astrophys. J.* **2011**, *743*, 46.
174. Martin, C.L.; Shapley, A.E.; Coil, A.L.; Kornei, K.A.; Murray, N.; Pancoast, A. Scattered Emission from z ~1 Galactic Outflows. *Astrophys. J.* **2013**, *770*, 41.
175. Pettini, M.; Rix, S.A.; Steidel, C.C.; Adelberger, K.L.; Hunt, M.P.; Shapley, A.E. New Observations of the Interstellar Medium in the Lyman Break Galaxy MS 1512-cB58. *Astrophys. J.* **2002**, *569*, 742–757.
176. Jones, T.; Stark, D.P.; Ellis, R.S. Dust in the Wind: Composition and Kinematics of Galaxy Outflows at the Peak Epoch of Star Formation. *Astrophys. J.* **2018**, *863*, 191.
177. Tremonti, C.A.; Moustakas, J.; Diamond-Stanic, A.M. The Discovery of 1000 km s^{-1} Outflows in Massive Poststarburst Galaxies at z=0.6. *Astrophys. J.* **2007**, *663*, L77–L80.
178. Diamond-Stanic, A.M.; Moustakas, J.; Tremonti, C.A.; Coil, A.L.; Hickox, R.C.; Robaina, A.R.; Rudnick, G.H.; Sell, P.H. High-velocity Outflows without AGN Feedback: Eddington-limited Star Formation in Compact Massive Galaxies. *Astrophys. J.* **2012**, *755*, L26.
179. Kacprzak, G.G.; Churchill, C.W.; Nielsen, N.M. Tracing Outflows and Accretion: A Bimodal Azimuthal Dependence of Mg II Absorption. *Astrophys. J.* **2012**, *760*, L7.
180. Kacprzak, G.G.; Muzahid, S.; Churchill, C.W.; Nielsen, N.M.; Charlton, J.C. The Azimuthal Dependence of Outflows and Accretion Detected Using O VI Absorption. *Astrophys. J.* **2015**, *815*, 22.
181. Bouché, N.; Hohensee, W.; Vargas, R.; Kacprzak, G.G.; Martin, C.L.; Cooke, J.; Churchill, C.W. Physical properties of galactic winds using background quasars. *Mon. Not. R. Astron. Soc.* **2012**, *426*, 801–815.
182. Schroetter, I.; Bouché, N.; Péroux, C.; Murphy, M.T.; Contini, T.; Finley, H. The VLT SINFONI Mg II Program for Line Emitters (SIMPLE). II. Background Quasars Probing Z ~1 Galactic Winds. *Astrophys. J.* **2015**, *804*, 83.
183. Muzahid, S.; Kacprzak, G.G.; Churchill, C.W.; Charlton, J.C.; Nielsen, N.M.; Mathes, N.L.; Trujillo-Gomez, S. An Extreme Metallicity, Large-scale Outflow from a Star-forming Galaxy at z ~0.4. *Astrophys. J.* **2015**, *811*, 132.
184. Erb, D.K. Feedback in low-mass galaxies in the early Universe. *Nature* **2015**, *523*, 169–176.
185. Hashimoto, T.; Ouchi, M.; Shimasaku, K.; Ono, Y.; Nakajima, K.; Rauch, M.; Lee, J.; Okamura, S. Gas Motion Study of Lyα Emitters at z ~2 Using FUV and Optical Spectral Lines. *Astrophys. J.* **2013**, *765*, 70.
186. Shibuya, T.; Ouchi, M.; Nakajima, K.; Hashimoto, T.; Ono, Y.; Rauch, M.; Gauthier, J.R.; Shimasaku, K.; Goto, R.; Mori, M.; et al. What is the Physical Origin of Strong Lyα Emission? II. Gas Kinematics and Distribution of Lyα Emitters. *Astrophys. J.* **2014**, *788*, 74.
187. Erb, D.K.; Steidel, C.C.; Trainor, R.F.; Bogosavljević, M.; Shapley, A.E.; Nestor, D.B.; Kulas, K.R.; Law, D.R.; Strom, A.L.; Rudie, G.C.; et al. The Lyα Properties of Faint Galaxies at z ~2-3 with Systemic Redshifts and Velocity Dispersions from Keck-MOSFIRE. *Astrophys. J.* **2014**, *795*, 33.

188. Geach, J.E.; Tremonti, C.; Diamond-Stanic, A.M.; Sell, P.H.; Kepley, A.A.; Coil, A.L.; Rudnick, G.; Hickox, R.C.; Moustakas, J.; Yang, Y. Violent Quenching: Molecular Gas Blown to 1000 km s^{-1} during a Major Merger. *Astrophys. J.* **2018**, *864*, L1.
189. George, R.D.; Ivison, R.J.; Smail, I.; Swinbank, A.M.; Hopwood, R.; Stanley, F.; Swinyard, B.M.; Valtchanov, I.; Werf, P.V. Herschel reveals a molecular outflow in a z = 2.3 ULIRG. *Mon. Not. R. Astron. Soc.* **2014**, *442*, 1877–1883.
190. Falgarone, E.; Zwaan, M.A.; Godard, B.; Bergin, E.; Ivison, R.J.; Andreani, P.M.; Bournaud, F.; Bussmann, R.S.; Elbaz, D.; Omont, A.; et al. Large turbulent reservoirs of cold molecular gas around high-redshift starburst galaxies. *Nature* **2017**, *548*, 430–433.
191. Gallerani, S.; Pallottini, A.; Feruglio, C.; Ferrara, A.; Maiolino, R.; Vallini, L.; Riechers, D.A.; Pavesi, R. ALMA suggests outflows in z 5.5 galaxies. *Mon. Not. R. Astron. Soc.* **2018**, *473*, 1909–1917.
192. Spilker, J.S.; Aravena, M.; Béthermin, M.; Chapman, S.C.; Chen, C.C.; Cunningham, D.J.M.; De Breuck, C.; Dong, C.; Gonzalez, A.H.; Hayward, C.C.; et al. Fast molecular outflow from a dusty star-forming galaxy in the early Universe. *Science* **2018**, *361*, 1016–1019.
193. Bryant, J.J.; Bland-Hawthorn, J.; Lawrence, J.; Croom, S.; Brown, D.; Venkatesan, S.; Gillingham, P.R.; Zhelem, R.; Content, R.; Saunders, W.; et al. Hector: A new massively multiplexed IFU instrument for the Anglo-Australian Telescope. In Proceedings of the Ground-based and Airborne Instrumentation for Astronomy VI, Edinburgh, UK, 26 June–1 July 2016; Volume 9908, p. 99081F.
194. Kepley, A.A.; Mühle, S.; Everett, J.; Zweibel, E.G.; Wilcots, E.M.; Klein, U. The Role of the Magnetic Field in the Interstellar Medium of the Post- Starburst Dwarf Irregular Galaxy NGC 1569. *Astrophys. J.* **2010**, *712*, 536–557.
195. Leslie, S.K.; Bryant, J.J.; Ho, I.T.; Sadler, E.M.; Medling, A.M.; Groves, B.; Kewley, L.J.; Bland-Hawthorn, J.; Croom, S.M.; Wong, O.I.; et al. The SAMI Galaxy Survey: Disc-halo interactions in radio-selected star-forming galaxies. *Mon. Not. R. Astron. Soc.* **2017**, *471*, 2438–2452.
196. Ramírez-Olivencia, N.; Varenius, E.; Pérez-Torres, M.; Alberdi, A.; Pérez, E.; Alonso-Herrero, A.; Deller, A.; Herrero-Illana, R.; Moldón, J.; Barcos-Muñoz, L.; et al. Sub-arcsecond imaging of Arp 299-A at 150 MHz with LOFAR: Evidence for a starburst-driven outflow. *Astron. Astrophys.* **2018**, *610*, L18.
197. O'Sullivan, E.; Zezas, A.; Vrtilek, J.M.; Giacintucci, S.; Trevisan, M.; David, L.P.; Ponman, T.J.; Mamon, G.A.; Raychaudhury, S. Deep Chandra Observations of HCG 16. I. Active Nuclei, Star Formation, and Galactic Winds. *Astrophys. J.* **2014**, *793*, 73.
198. McQuinn, K.B.W.; Skillman, E.D.; Heilman, T.N.; Mitchell, N.P.; Kelley, T. Galactic outflows, star formation histories, and time-scales in starburst dwarf galaxies from STARBIRDS. *Mon. Not. R. Astron. Soc.* **2018**, *477*, 3164–3177.



© 2018 by the author. Licensee MDPI, Basel, Switzerland. This article is an open access article distributed under the terms and conditions of the Creative Commons Attribution (CC BY) license (http://creativecommons.org/licenses/by/4.0/).